

Ultrafast magnetization reversal in ferromagnetic spin valves: An s - d model perspectiveQuentin Remy **Cavendish Laboratory, University of Cambridge, Cambridge, United Kingdom
and Université de Lorraine, CNRS, IJL, F-54000 Nancy, France*

(Received 10 March 2023; revised 9 May 2023; accepted 16 May 2023; published 30 May 2023)

We present an extension to simple s - d models, aiming at simulating ultrafast magnetization dynamics and spin transport in metallic heterostructures. In particular, we consider an alternative spin dissipation channel due to a finite exchange splitting of the s band. From this theory, we show three different mechanisms governing the dynamics of spin accumulation. On top of the already widely discussed “ $-dM/dt$ ” electron-magnon mechanism, we study the role of a dynamic change of exchange splitting (of conduction electrons) as well as the rotation of spins reflected at an interface with a ferromagnet. Finally, we use the presented theory to explain the recent observation of subpicosecond reversal of a ferromagnet in rare-earth free spin valves. Our conclusion agrees with the one of J. Igarashi *et al.* [*Nat. Mater.* (2023)] favoring magnetization reversal due to the rotation of the spin polarization of a reflected spin current.

DOI: [10.1103/PhysRevB.107.174431](https://doi.org/10.1103/PhysRevB.107.174431)**I. INTRODUCTION**

Ever since the first investigations of ultrafast magnetization dynamics of metals [1–6], numerous and diversified theoretical approaches have been attempted to understand its origin [7]. The proposed contributing microscopic mechanisms are typically classified as spin transport [8–14], spin-flip scattering [12,15–18], and magnon generation [19–23] processes. A sharp separation of the latter two mechanisms is, however, not always clear, mostly because the magnon generation mechanism is generally discussed in the framework of the electron-magnon interaction [21,24] where the creation of a magnon always comes with a spin flip, and also because both magnons and spin flips (Stoner excitations) are two specific cases of magnetic excitation [25,26]. Assuming a clear separation between both types of excitation is possible, recent experimental results seem to confirm that both magnon generation and spin flips are happening during ultrafast demagnetization (UDM) [27,28] and the final destination of angular momentum during magnetization quenching is the crystal lattice [29]. The generation of circularly polarized phonons was also observed for nickel [30]. A transfer to the electromagnetic field has been estimated negligible [31,32] and a possible transient role of the orbital degree of freedom [33] via, for instance, an increase of the orbital angular momentum [19,34], still has not been observed to the best of our knowledge. Theoretical works, however, indicate that such an increase cannot be observed because orbital

angular momentum in metals is transferred to the lattice with a characteristic time around 1 fs [35,36]. The computational frameworks that can incorporate some or all of these processes include the real-time time-dependent density functional theory (rt-TDDFT) [14,34,37–42], a direct propagation of the system wave function with a parametrized many-body Hamiltonian [35,36,43,44], the semiclassical Boltzmann equation [8,9,17,21–23,45–53], quantum kinetics [18,54–56], molecular dynamics [57,58], the stochastic atomistic Landau-Lifshitz-Gilbert equation [58–61], the Landau-Lifshitz-Bloch equations [62,63], as well as other more phenomenological parametrized models [64] such as the so-called three-temperature model (3TM) [3] and its various extensions [15,20,65–68]. We note that in parametrized approaches, parameters may be obtained from *ab initio* calculations [16,69–72]. In particular, recent works seem to validate the use of temperature-based models for a description of magnetization dynamics [58,60,61,67] provided that one properly accounts for energy conservation and the temperature dependence of all parameters. Because there is so far no method that is able to completely solve the problem of UDM of metals for all relevant spatial scales and timescales, such simplified thermal *bath* models prove to be quite useful. However, it is important to note that such models are not suitable to describe short timescale effects, i.e., effects arising before each degree of freedom of interest can be described as a thermal bath.

Moreover, the field of ultrafast magnetization dynamics in metals is not limited to UDM. A plethora of consequent phenomena have been observed such as all-optical magnetization switching [73–75], ultrafast spin injection [12,64,76–85], terahertz electromagnetic pulse emission [64,78,86,87], ultrafast spin-transfer torque [84,88,89], and magnetization reversal of ferromagnets using nonlocal transfer of spin [90–94] or spin-orbit torque [95]. We also note the apparent thermal and incoherent nature of these phenomena as experimentally highlighted by the fact that they do not intrinsically depend

*Corresponding author: quentinremy5@gmail.com

on the external energy stimulus used to trigger the dynamics [96–99]. Thus, the simplified parametrized models can be applied to study or predict more complex magnetization dynamics subsequent to UDM. It is also easier to enforce angular momentum conservation (although in a more phenomenological way), which is believed to not always be satisfied in more complicated approaches such as rt-TDDFT [100].

In this work, we use a simple reservoir approach for the dynamics and transport of both energy and angular momentum, presented in Sec. II, which is suitable for the study of ultrafast thermal effects in metallic multilayers with possibly several magnetic layers. It is based on an s - d model which can incorporate both transverse (\sim magnons) and longitudinal (spin flips) magnetic excitations. In particular, this framework allows us to simulate a more complex spin accumulation dynamics which could explain recent experiments [92,101]. Simulations of UDM and spin accumulation generation in systems with a single magnetic layer are briefly shown in Sec. III. Then, magnetization reversal in ferromagnetic spin valves is discussed in Sec. IV. We conclude and discuss possible improvements in Sec. V.

II. MODEL

In order to provide some general context, we start the description of our model with a general model Hamiltonian \mathcal{H} suitable for an s - d model, in the absence of any external field and for a homogeneous material, where itinerant (s) electrons, phonons (p), and localized (d) electrons are distinct quantities defined by their respective free (quasi)particle Hamiltonian terms \mathcal{H}_e , \mathcal{H}_p , and \mathcal{H}_d :

$$\mathcal{H} = \mathcal{H}_e + \mathcal{H}_p + \mathcal{H}_d + \mathcal{H}_{ep} + \mathcal{H}_{ed} \quad (1)$$

together with two interaction terms \mathcal{H}_{ep} and \mathcal{H}_{ed} for the electron-phonon and s - d interactions, respectively. Two important approximations of this model are (i) d states are localized (they all have the same energy for a given spin quantum number) and are not hybridized with s states and (ii) d states do not contribute to (heat and charge) transport. The real impact of these approximations on the simulated dynamics is unclear since the final equations rely on parameters whose input values are often taken from experiments or *ab initio* calculations that do not make these approximations. We write the s - d interaction term as [99,102,103]

$$\mathcal{H}_{ed} = -J \sum_i \left[\frac{1}{2} (\hat{S}_i^+ \hat{s}_i^- + \hat{S}_i^- \hat{s}_i^+) + \hat{S}_i^z \hat{s}_i^z \right], \quad (2)$$

where $J > 0$ is the s - d interaction constant for ferromagnetic coupling between s and d electrons, $\hat{S}_i = (\hat{S}_i^x, \hat{S}_i^y, \hat{S}_i^z)$ are the spin operators for d electrons localized on lattice site i , $\hat{s}_i = \frac{1}{2} \hat{c}_i^\dagger \boldsymbol{\sigma} \hat{c}_i$ are the spin operators for s electrons with $\hat{c}_{i\sigma}^\dagger$ and $\hat{c}_{i\sigma}$ the creation and annihilation operators for a Wannier state at lattice site i and spin σ , and $\boldsymbol{\sigma} = (\sigma^x, \sigma^y, \sigma^z)$ is the vector of Pauli matrices. Superscripts $+$ and $-$ denote ladder operators as usual, for instance, $\hat{S}_i^\pm = \hat{S}_i^x \pm i \hat{S}_i^y$. The term with the z components is treated in the mean field approximation [102,103] and we write the average (over all quantum states and lattice sites) of the z components of the itinerant and localized spin operators as s^z and S^z , respectively. These two quantities contain all the angular momentum, per atom in units

of \hbar , possessed by electrons within the mean field approximation. The Hamiltonian then becomes

$$\mathcal{H} = \mathcal{H}'_e + \mathcal{H}_p + \mathcal{H}'_d + \mathcal{H}_{ep} + \mathcal{H}_{ed}^\pm, \quad (3a)$$

$$\mathcal{H}'_e = \mathcal{H}_e - JS^z \sum_k \frac{1}{2} (\hat{c}_{k\uparrow}^\dagger \hat{c}_{k\uparrow} - \hat{c}_{k\downarrow}^\dagger \hat{c}_{k\downarrow}), \quad (3b)$$

$$\mathcal{H}'_d = \mathcal{H}_d - JS^z \sum_i \hat{S}_i^z, \quad (3c)$$

$$\mathcal{H}_{ed}^\pm = -J \sum_i \frac{1}{2} (\hat{S}_i^+ \hat{s}_i^- + \hat{S}_i^- \hat{s}_i^+), \quad (3d)$$

where we wrote the mean field term felt by the s electrons in the Bloch representation (with states indexed by a wave vector \mathbf{k}).

From this Hamiltonian, the system dynamics is obtained in the framework of perturbation theory: the interaction terms \mathcal{H}_{ep} and \mathcal{H}_{ed}^\pm are assumed to be much smaller than the free-particle terms. The interaction terms are then used to determine exchange of energy (as well as momentum and angular momentum) while the free-particle terms are used for conservation of energy (as well as momentum and angular momentum). Notably, the interaction energies are neglected in the conservation of energy, which is not true in general [99], but is valid whenever perturbation theory can be applied.

We first discuss how the free-particle terms are treated. The itinerant free-electron term \mathcal{H}'_e describes renormalized (for instance, due to the electron-phonon and electron-electron interactions) Bloch states which are assumed to be characterized by a thermal distribution for each (pure) spin state. The electronic temperature T_e is assumed to be the same for both spin species $\sigma = \pm \frac{1}{2}$ while the chemical potential μ_σ and the density of states D_σ are different for different spins. The mean field term in Eq. (3b) adds an exchange splitting to the s band. Noting E_σ^0 the lowest energy of the s band, the exchange splitting is seen to be $E_\uparrow^0 - E_\downarrow^0 = -JS^z$. The free-phonon term \mathcal{H}_p represents renormalized phonons [104] described as Debye phonons in equilibrium at a temperature T_p . The localized electrons term \mathcal{H}_d can contain contributions due to d - d exchange interaction, magnetocrystalline anisotropy, and dipolar interaction [22]. It is also treated within the mean field approximation [51]. We consider for simplicity the case where the spin quantum number S of the d electrons is $\frac{1}{2}$. The total mean field, including the one generated by the s - d interaction (second term of Eq. (3c)), induces an energy splitting $\Delta = 2mk_B T_C$ between the d electrons energy levels where $m = -2S^z$ is the magnetization of the d electrons normalized to its zero-temperature value and T_C is the Curie temperature of the ferromagnetic layer. We note that the d electrons are not assumed to be in internal equilibrium (in the d electrons bath itself) for a general value of S , but for $S = \frac{1}{2}$, in this mean field approximation, there is no difference between internal equilibrium and out of equilibrium [94]. It is also worth noting that the mean field approximation for localized spins predicts an energy splitting $\Delta \sim 0.1$ eV while the exchange splitting of d states in transition metals is of the order of 1 eV. Solving this issue would require a better description of d electrons, which is beyond the scope of this work.

The electron-phonon term \mathcal{H}_{ep} is treated in perturbation theory via Fermi's golden rule [104–106]. We consider the usual high-temperature case where the energy transfer between electrons and phonons is found to be $g_{ep}(T_e - T_p)$ with g_{ep} the electron-phonon coupling considered as temperature independent. We also consider that this term induces angular momentum transfer between the s electrons and the lattice and which is phenomenologically given by, following Refs. [102,103], $(s^z - s_{ie}^z)/\tau_s$ with τ_s a spin relaxation time. The instantaneous equilibrium s electrons spin polarization s_{ie}^z is defined such that $s^z - s_{ie}^z$ is the excess of spin due to the out-of-equilibrium state of the itinerant electrons [22]. It is discussed below. The exchange of energy due to the s - d interaction term \mathcal{H}_{ed}^\pm is obtained via a slightly generalized version of Fermi's golden rule [51,102,107] which leads to a typical two-level dynamics [15,51,108]:

$$\frac{dm}{dt} = \frac{1}{\tau_m} \left(m - \frac{\Delta\mu}{2k_B T_C} \right) \left[1 - m \coth \left(\frac{2mk_B T_C - \Delta\mu}{2k_B T_e} \right) \right], \quad (4)$$

where τ_m is the characteristic time for angular momentum transfer from d to s electrons, which needs to be taken as an additional parameter [51,99], and $\Delta\mu = \mu_\uparrow - \mu_\downarrow$ is the spin accumulation of the s electrons. The spin accumulation defined in this way is a central quantity in the s - d model as used in previous works [22,51,102,103]. It contains part of the information needed to describe the total angular momentum stored in s electrons [see Eq. (8) below]. The spin-averaged chemical potential $\mu = (\mu_\uparrow + \mu_\downarrow)/2$ is also a dynamic quantity as given by Eq. (A6), but it is not a central quantity in this work.

The equations governing the dynamics of the system come from the fact that conservation equations must be fulfilled while transfers happen as given by interactions, which we just discussed. We only focus on energy and angular momentum conservation equations, and discard effects appearing when one also considers charge [66] and momentum [109] conservation, as we wish to discuss new effects arising from angular momentum conservation driven by energy transfer. The energy conservation equation for the total Hamiltonian (1) reads as

$$\frac{\partial}{\partial t} \left(\frac{\gamma}{2} T_e^2 + C_p T_p - \rho m \frac{\Delta}{2} \right) + \nabla \cdot (\mathbf{Q}_e + \mathbf{Q}_p) = 0, \quad (5)$$

where we chose the middle of both d electron levels as the reference energy for d electrons, ρ is the number of atoms per unit volume, γT_e is the standard expression for a free-electron gas volumetric heat capacity, C_p is the phonon volumetric heat capacity, and \mathbf{Q}_e and \mathbf{Q}_p are the electronic and phononic heat current densities, respectively. The phononic heat current is given by the standard Fourier's law $\mathbf{Q}_p = -\kappa_p \nabla T_p$, with κ_p the phonon heat conductivity, while the electronic heat current is given by $\mathbf{Q}_e = -\kappa_e (T_e/T_p) \nabla T_e$ with κ_e the equilibrium (when the electronic plus phononic system is in equilibrium) electronic heat conductivity. Such a description of the energy flow within electrons and phonons was recently used to successfully describe the ultrafast strain dynamics of heterostructures similar to the ones considered in our work [110]. As mentioned above, d states do not contribute

to heat transport in this model, and so possible magnonic heat currents do not appear in Eq. (5). The resulting heat equations for the system, modeled as one dimensional in the thin-film limit, are

$$\gamma T_e \frac{\partial T_e}{\partial t} = \frac{\partial}{\partial z} \left(\kappa_e \frac{T_e}{T_p} \frac{\partial T_e}{\partial z} \right) - g_{ep}(T_e - T_p) + 2\rho m k_B T_C \frac{dm}{dt} + S(z, t), \quad (6a)$$

$$C_p \frac{\partial T_p}{\partial t} = \kappa_p \frac{\partial^2 T_p}{\partial z^2} + g_{ep}(T_e - T_p). \quad (6b)$$

The energy dynamics for the d electrons is given by Eq. (4) since there is a one-to-one relationship between the energy density $-\rho m \Delta/2$ and the absolute value of magnetization $|m|$ in this model. The magnetization-dependent term in Eq. (6a) [67,111] comes from the requirement that Eq. (5) must be fulfilled. The last term in Eq. (6a) is due to energy transfer from an external laser pulse as computed in [112] where it is argued that energy conservation in the total system, including the electromagnetic field, is significantly broken. Satisfying conservation of energy when the electromagnetic field is included is, however, irrelevant to the phenomena discussed in this work and beyond the scope of this work [113].

The angular momentum conservation equation is

$$\frac{\partial}{\partial t} (s^z + S^z + S_p^z) + \nabla \cdot \mathbf{J}_s = 0. \quad (7)$$

Similarly to energy conservation, quantities appearing after the time derivative operator are intensive quantities. In this case we take them as angular momentum (or spin polarization for the electrons) per atom in units of \hbar to have notations consistent with the previously introduced averaged spins. S_p^z refers to the angular momentum dissipated in the lattice which, according to our previous discussion, satisfies $\partial S_p^z / \partial t = (s^z - s_{ie}^z)/\tau_s$. \mathbf{J}_s is the spin current density and we neglect a contribution to this current density due to angular momentum transport in the localized d electrons [23,114] or in phonons [115]. Moreover, we assume that spin transport only happens via conduction electrons close to the Fermi level [53] and so depends on the spin accumulation only [51,64,84]. We will detail the spin current term when we use it in Sec. IV.

To close our system of equations, and because spin transport depends on the spin accumulation, we need to rewrite Eq. (7) in terms of $\Delta\mu$. The relation we need is [22,49]

$$s^z - s_{ie}^z = \bar{D}(\Delta\mu - \delta), \quad (8)$$

which is valid to first order in both the spin accumulation $\Delta\mu$ and the change of exchange splitting $\delta = -J(S^z - S_{ie}^z)$ with S_{ie}^z the instantaneous equilibrium value of S^z . $\bar{D} = D_\uparrow(\varepsilon_F) D_\downarrow(\varepsilon_F) / [D_\uparrow(\varepsilon_F) + D_\downarrow(\varepsilon_F)]$, with ε_F the equilibrium Fermi level and N the total number of s electrons, and it is taken as a parameter [22,51]. A derivation of Eq. (8) is provided in Appendix A. This equation also allows us to consider the change of exchange splitting in the conduction electrons which was argued to be fundamental to describe ultrafast magnetization dynamics of itinerant ferromagnets [49,116] and later considered in both itinerant and localized electrons [22]. We also need to calculate the instantaneous equilibrium values of s^z and S^z . For s_{ie}^z , we follow the argumentation of

Gridnev [103], simplified to the case of ferromagnets:

$$s_{ic}^z(t) = \chi S^z(t) \quad (9)$$

with χ a spin susceptibility. When ferromagnetic order only arises due to the s - d interaction, $\chi = 4k_B T_C / J$. The choice of $S_{ic}^z(t)$ is more complicated. The naive case where $S_{ic}^z(t)$ is given by its equilibrium value for a temperature given by the electronic temperature at the instant of interest $T_e(t)$ would be unphysical. In particular, it would lead to a fast change (even a discontinuity in the mean field approximation) of the slope of the spin accumulation dynamics curve when the electronic temperature crosses the Curie temperature. Rather, we follow the physics of out-of-equilibrium spin relaxation, where the dynamics of localized spins for $S = \frac{1}{2}$ is governed by an equation with the following form [15,51,94,108]:

$$\frac{dm}{dt}_{\text{relaxation}} = -\frac{m(t) - m_{ie}(t)}{\tau(t)}, \quad (10a)$$

$$m_{ie}(t) = -2S_{ic}^z(t) \equiv \tanh\left(\frac{2k_B T_C m(t) - \Delta\mu(t)}{2k_B T_e(t)}\right), \quad (10b)$$

where $\tau(t)$ is a characteristic time that depends on time and, in general, $\Delta\mu$ represents an energy splitting due to an external (to the d electrons subsystem) source of angular momentum. For instance, for the s - d model [51] fundamentally describing, at each instant t , spin relaxation of d electrons in the thermal bath of s electrons

$$\tau(t) = \frac{m_{ie}(t)\tau_m}{m(t) - \Delta\mu(t)/(2k_B T_C)}, \quad (11)$$

while for Elliott-Yafet scattering as computed by Koopmans *et al.* [15]

$$\tau(t) = \frac{m_{ie}(t)T_C}{m(t)RT_p(t)} \quad (12)$$

with R the demagnetization rate in the Elliot-Yafet model [15] and an external source of angular momentum can also be considered [117]. Equation (10a) is more general than a Bloch equation, and even more general than (the longitudinal term of) the self-consistent Bloch equation [118,119] because τ depends on time in a complicated way. Here we keep $\tau(t) = \tau_s$ which is consistent with the naive description of spin dissipation (7) [102,103] and the self-consistent Bloch equation [118,119].

Using Eqs. (8) and (9), Eq. (7) becomes [99]

$$\begin{aligned} \frac{d\Delta\mu}{dt} = & \left(\frac{S}{D}(1 + \chi) + JS\right) \frac{dm}{dt} - JS \frac{dm_{ie}}{dt} \\ & - \frac{\nabla \cdot \mathbf{J}_s}{D} - \frac{\Delta\mu}{\tau_s} + JS \frac{m - m_{ie}}{\tau_s} \end{aligned} \quad (13)$$

which together with Eqs. (4), (6), and (10b) form the set of equations we wish to solve to obtain the dynamics of T_e , T_p , m , and $\Delta\mu$. Other quantities such as the exchange splitting or the total spin polarization in the electronic subsystem can be obtained from the latter four quantities. Equation (13) is valid for any value of S but more equations are then needed to calculate the dynamics of m and m_{ie} . Equation (13) generalizes previous approaches [51,103] mainly because it includes a dynamic exchange splitting of the s electrons (terms proportional to

JS). It also includes an equilibrium spin polarization of these electrons which was not in the model of Beens *et al.* [51]. This dynamic exchange splitting was considered before by Tveten *et al.* [22] and we note a similarity between the form of our Eqs. (4) and (13) and Eqs. (5) and (4) of Ref. [22] if one replaces m and m_{ie} by the out-of-equilibrium and equilibrium (Bose-Einstein) magnon distribution, respectively. The system of equations of Tveten *et al.* is, however, much more complicated than ours to solve and it is also not clear whether the magnonic description of the magnetization dynamics via the Holstein-Primakoff expansion is valid especially since we wish to model situations where magnetization can be fully quenched or even reversed [120]. Finally, a mechanism appearing in our approach is a spin dissipation in the lattice due to a nonzero value of the out-of-equilibrium magnetization $m - m_{ie}$ of d electrons. All previous works so far (in this framework) have, as far as we know, only been considering a spin dissipation due to the presence of a spin accumulation as defined above. Within the context of the derivation of Eq. (8), this means that we consider spin relaxation in the lattice due to a spin nonequilibrium in s electrons close to the Fermi level (the spin accumulation dissipation term $-\Delta\mu/\tau_s$) as well as all the other ones (the dynamic exchange splitting dissipation term $JS(m - m_{ie})/\tau_s$). This additional contribution comes from the fact that all electronic states are considered to contribute to the spin dissipation when the phenomenological term $\partial S_p^z / \partial t = (s^z - s_{ic}^z) / \tau_s$ [102,103] is assumed. It was argued, in a different framework, that a relaxation-time approximation can be used to simulate UDM, with a relaxation time identical for all electronic states [52]. One potential interesting consequence of this additional term is that it can change the sign of the spin accumulation as compared to what can be expected from the usual “ $-dM/dt$ ” law for the spin generation rate (first term on the right-hand side of Eq. (13)) since when dm/dt is negative, $m - m_{ie}$ is usually positive (this depends on the dynamics of the electronic temperature and the spin accumulation). Also note that, even though Eq. (4) can be written as Eq. (10a), dm/dt is not proportional (as a function of time) to $m - m_{ie}$ due to the complex time dependence of τ .

In order to facilitate the numerical implementation of this model and to explain its limitations, it is instructive to expand Eq. (13) using Eq. (10b):

$$\begin{aligned} \frac{d\Delta\mu}{dt} = & \frac{1}{1 - \frac{JS\eta(t)}{2k_B T_e(t)}} \left\{ \left[\frac{S}{D}(1 + \chi) + JS \left(1 - \eta(t) \frac{T_C}{T_e(t)}\right) \right] \frac{dm}{dt} \right. \\ & + \frac{JS\eta(t)\xi(t)}{T_e(t)} \frac{dT_e}{dt} - \frac{\nabla \cdot \mathbf{J}_s}{D} - \frac{\Delta\mu(t)}{\tau_s} \\ & \left. + \alpha JS \frac{m(t) - m_{ie}(t)}{\tau_s} \right\}, \end{aligned} \quad (14a)$$

$$\eta(t) \equiv \text{sech}^2[\xi(t)]; \quad \xi(t) \equiv \frac{2k_B T_C m(t) - \Delta\mu(t)}{2k_B T_e(t)}. \quad (14b)$$

Additional terms appear due to the dependence of m_{ie} on T_e , m , and $\Delta\mu$. These terms are proportional to the quantity η which becomes sizable when ξ is small, i.e., at large electronic temperature and for values of magnetization where effects such as spin cooling and spin heating [94] are expected to become significant (when $2k_B T_C m(t) \sim \Delta\mu(t)$). Moreover,

we notice that the change of spin accumulation diverges when $[JS\eta(t)]/[2k_B T_e(t)] \sim 1$, which may happen even when ξ is large depending on the complexity of the dynamics of T_e , m , and $\Delta\mu$. This divergence happens when the first-order expansions of the density of states of s electrons leading to Eq. (8) are no longer valid approximations. These approximations are valid as long as $J \ll 1/\bar{D}$ (see Appendix A). This is consistent with the fact [51,121] that the width of the conduction band is usually larger than JS . The terms proportional to J should then be treated as a correction to the model of Beens *et al.* [51], however, we will show that they can significantly change the magnetization dynamics when $dm/dt \sim 0$ in the presence of an external source of spin accumulation. Equation (14a) not only shows that the spin accumulation and the spin current are not always proportional to $-dm/dt$ [23] but the spin generation rate itself [79] is also not always proportional to $-dm/dt$ due to the dynamic exchange splitting. We introduced a parameter α which is equal to 1 in our model but we will also set it to 0 in the next section to see the effect of the corresponding term in Eq. (14a).

Because both s and d electrons carry angular momentum in this model, even at equilibrium, the question arises as to which quantity is measured in experiments. Indeed, it is not clear whether an optical probe measuring magnetization via magneto-optical effects would be as sensitive to both kinds of electrons or not. Here we will assume that the experimentally measured quantity is proportional to the total spin angular momentum of the system as we are only interested in qualitative modeling. Then a magnetic signal will be proportional to

$$\begin{aligned} -S_{\text{tot}}^z &\equiv -(S^z + s^z) \\ &= S[m(1 + \chi) + J\bar{D}(m - m_{\text{ie}})] - \bar{D}\Delta\mu. \end{aligned} \quad (15)$$

Showing that even under our simple approximation (9), the signal will not be proportional to the d electrons' normalized magnetization m due to a nonzero spin accumulation [51] and dynamic exchange splitting. All the data we plot are normalized by the equilibrium spin angular momentum $-Sm(1 + \chi)$ and we note the corresponding normalized magnetization m_{tot} . We discuss the separate dynamics of the (not normalized) spin angular momentum of s and d electrons in some specific cases in Appendix B.

The systems we wish to simulate are actually multilayers and are thus not homogeneous. We thus assume as usual that all the previous equations are valid within each layer of the multilayer. We solve the conservation of energy equation (5) by discretizing each layer and we use appropriate boundary conditions for each interface [66,99]. For the conservation of angular momentum, we assume that magnetization is constant along the thickness of each magnetic layer and use the average of the electronic temperature in the corresponding layer as the input temperature appearing in Eqs. (4) and (13). Thus, the term $2mk_B T_C dm/dt$ in Eq. (5) is identical for all depths in a given magnetic layer. Going beyond this approximation would require a generalization of this s - d model to include either a direct d - d coupling [122] or indirect s - d coupling between neighboring atomic layers. Such approach is beyond the scope of this work.

III. ULTRAFAST DEMAGNETIZATION OF A SINGLE LAYER

We first present results for a multilayer structure with a single ferromagnetic layer, namely, sapphire(substrate)/Ta(5)/Pt(4)/[Co/Pt](3.2)/Ta(5) similarly to Ref. [101] where numbers between brackets are thicknesses in nm and [Co/Pt] is a ferromagnetic multilayer which is simulated as an effectively homogeneous medium. We neglect spin transport in this case. We use a 50-fs (Gaussian) laser pulse, with normal incidence (coming from the sample side, i.e., the air/Ta interface) and 800-nm central wavelength to bring the system out of equilibrium. We study the dynamics of various quantities as a function of time delay with respect to the time instant where the position of the center of the laser pulse is at the air/Ta interface. The sample is initially at equilibrium with room temperature chosen to be 300 K. The parameters entering the energy conservation equation are taken from our previous works [92,94,99] and we choose $\rho = 7.5 \times 10^{28} \text{ m}^{-3}$ which lies between the values of pure Co ($\sim 9 \times 10^{28} \text{ m}^{-3}$) and Pt ($\sim 6.5 \times 10^{28} \text{ m}^{-3}$). For the angular momentum parameters we choose $\tau_m = 100$ fs, $\tau_s = 20$ fs, and $1/\bar{D} = 1$ eV as in [51]. We choose to study $\chi = 1$ such that Eq. (13) reduces to Eq. (6) of [51] when $J = 0$ eV since we have $S = \frac{1}{2}$. We also show some results for $\chi = 0.1$ in Appendix B and generally find that different values of this parameter do not qualitatively change the conclusions of our work. This is in agreement with Eqs. (14a) and (15) which show that different values of χ only change the efficiency of the spin generation rate due to the change of d electrons' magnetization and the ratio of s to d electrons' magnetizations, respectively. These parameters will be kept in the rest of this work. In this section, we choose $J = 0$ or 0.1 eV and $T_C = 700$ K. We will also study the effect of the newly proposed spin dissipation channel by using $\alpha = 0$ or 1. All the reported fluences are external fluences, i.e., not the absorbed ones.

Figure 1(a) shows the magnetization dynamics of the [Co/Pt] multilayer for various fluences. We recover the standard behavior, with an UDM followed by a "fast" recovery (where spins and electrons do not form an equilibrated sub-bath of the system) and a "slow" recovery (where spins and electrons are equilibrated and the dynamics is driven by the phonon temperature dynamics via heat dissipation in the substrate). At higher fluences, we also recover the so-called critical slowing down (CSD) of magnetization dynamics [15,20,59,62,94,118]. In Figs. 1(b)–1(d), we plot the normalized magnetization, temperatures, and spin accumulation, respectively, for four different models. All four models lead to qualitatively identical dynamics. A quantitative difference is observed for fluences such that there is a significant quenching of magnetization and yet at the same time a significant remagnetization. All four models lead to almost identical dynamics when there is a significant CSD (not shown). Neglecting the dynamic exchange splitting can change the value of the normalized magnetization by a few percent during the UDM and "fast" recovery phases. By only turning off the spin dissipation channel due to the dynamic exchange splitting, we recover almost the same

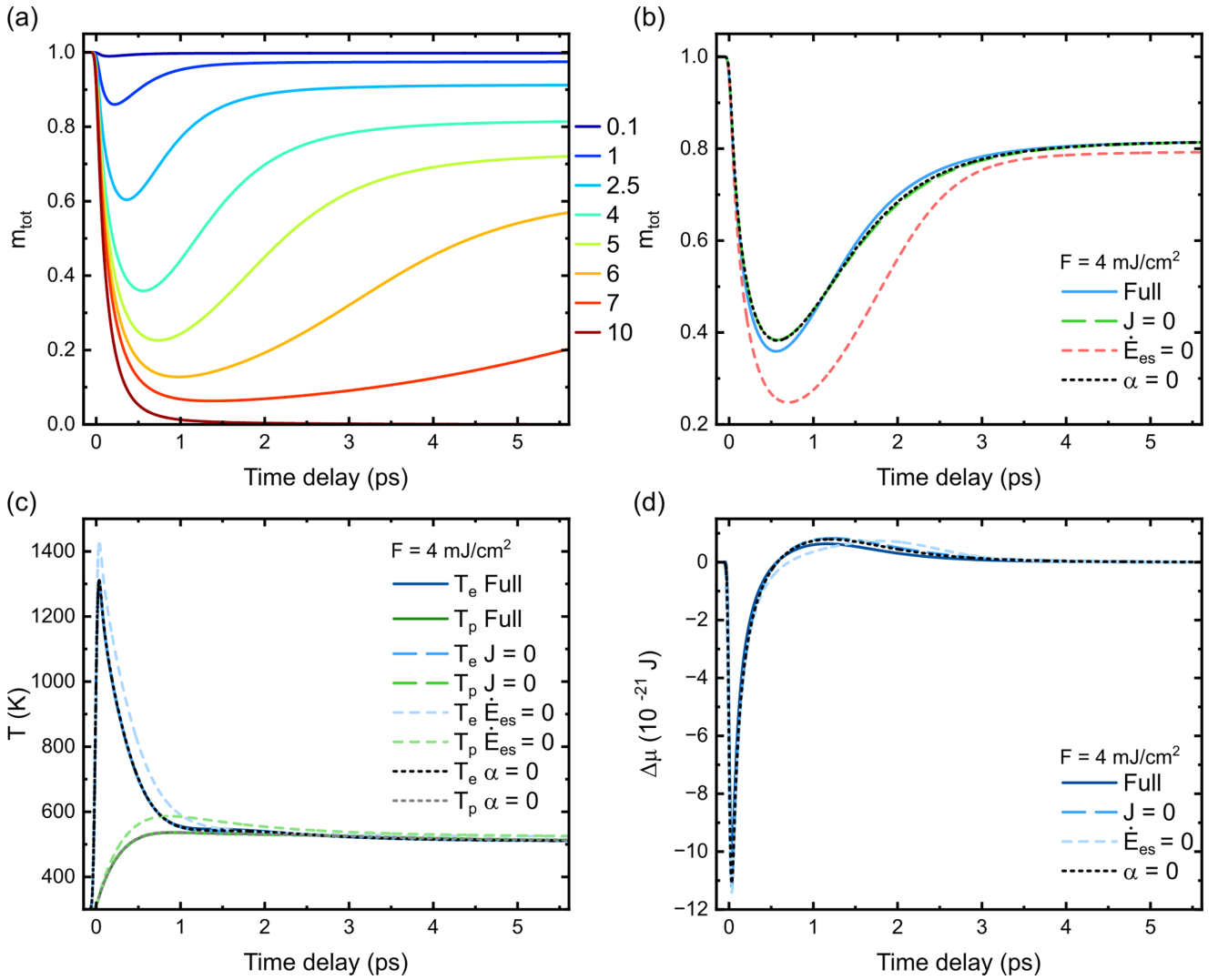


FIG. 1. (a) Normalized magnetization m_{tot} of the [Co/Pt] multilayer as a function of time delay for various fluences as noted on the right of the plot (in mJ/cm^2). (b) Comparison of the magnetization dynamics for a fluence of 4 mJ/cm^2 and different models; “Full” corresponds to the full equation (14a) with $J = 0.1 \text{ eV}$ and $\alpha = 1$; “ $J = 0$ ” is obtained by setting $J = 0 \text{ eV}$; “ $\dot{E}_{\text{es}} = 0$ ” is obtained by neglecting the magnetization-dependent term in Eq. (6a); “ $\alpha = 0$ ” is obtained by setting α to zero. (c) Same comparison as in (b) but for the electron and phonon temperature as indicated. (d) Same comparison as in (b) but for the spin accumulation as indicated.

dynamics as when we completely turn off the dynamic exchange splitting, indicating that the dissipation part dominates the dynamics induced by the dynamic exchange splitting. A bigger effect on the magnetization dynamics is obtained by turning off transfer of energy from d to s electrons. This is because it modifies the temperature dynamics as shown in Fig. 1(c).

Overall, we do not observe any drastic difference between the model of Beens *et al.* [51] and ours, even in the high-fluence limit. The reason is that, when $dm/dt \sim 0$ and so when terms proportional to J could dominate, the temperature dynamics is already much slower and the self-consistency of our system of equations forces $d\Delta\mu/dt \sim 0$. The situation will be completely different in the next section where an external source of angular momentum (due to an additional ferromagnetic layer) can also drive the spin accumulation dynamics.

IV. SUBPICOSECOND MAGNETIZATION SWITCHING IN FERROMAGNETIC SPIN VALVES

The aim of this section is to study potential mechanisms that can lead to the subpicosecond magnetization switching of ferromagnets observed in [101]. In this case, the system is sapphire(substrate)/Ta(5)/Pt(4)/[Co/Pt](7)/Cu(10)/[Co/Pt](3.2)/Ta(5) where the first [Co/Pt] multilayer (7 nm thick) is referred to as the “reference” layer and the second [Co/Pt] multilayer (3.2 nm thick) is referred to as the “free” layer. A magnetic configuration of the system where the magnetizations of each ferromagnetic multilayer are parallel is noted “P” and if they are antiparallel, we note it “AP.” The main result of Ref. [101] was to show that upon a single femtosecond laser pulse irradiation of the sample, the free layer can reverse its magnetization. For such a thickness of Cu, this can happen whether the sample is initially prepared in either a P or an AP configuration. However, less fluence

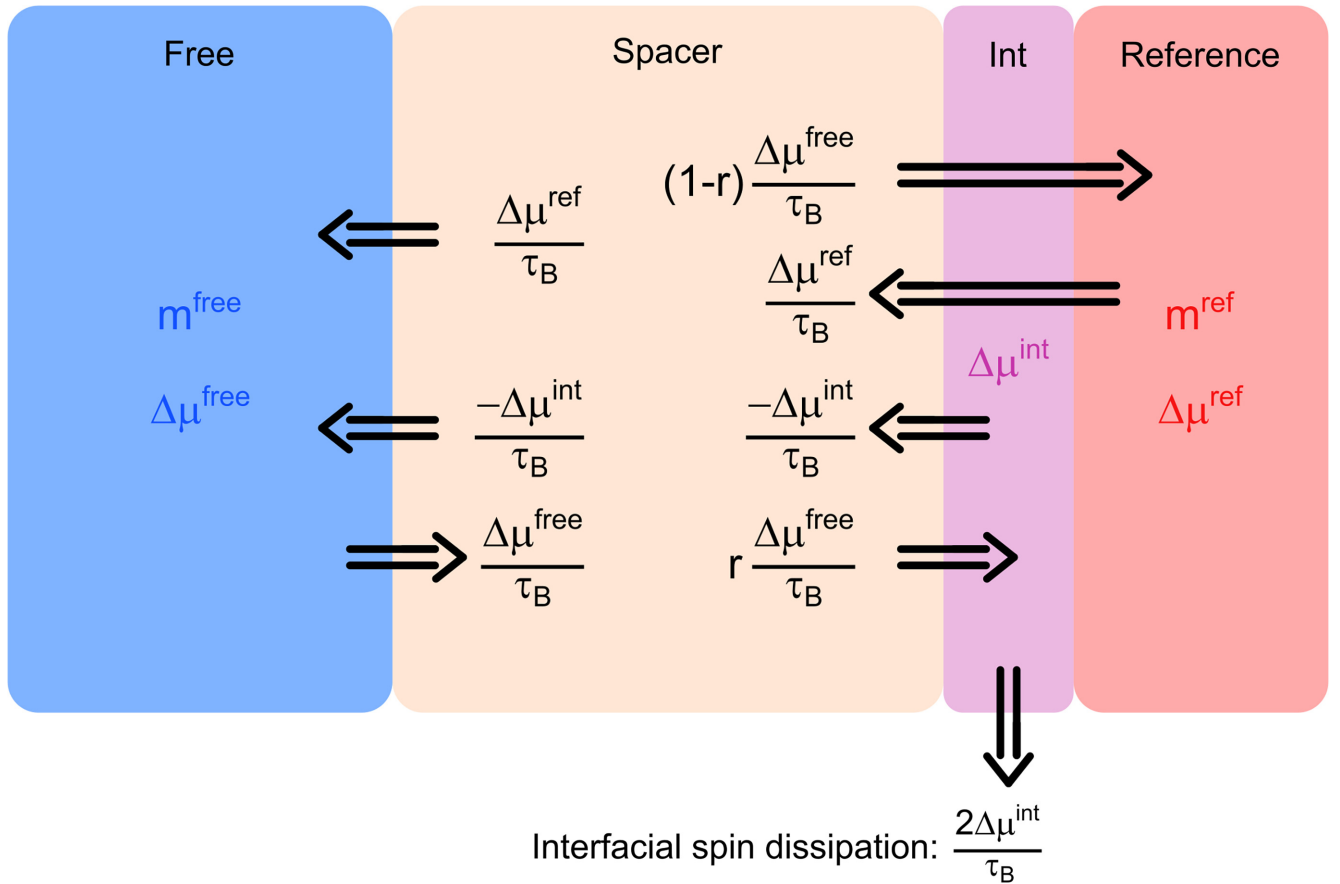


FIG. 2. Schematic description of the ballistic spin transport model. Black arrows represent the various spin currents considered at each interface. The corresponding terms in the spin transport equations (17) and (18) are shown next to each arrow. “Spacer” refers to the Cu spacer layer and “Int” to the Cu/reference layer interface.

is systematically required to reverse the magnetization of the free layer from a P configuration compared to the AP configuration. Also, the dynamics of the reversal was measured for an initial P configuration and the free-layer magnetization was seen to cross zero before the reference layer starts to remagnetize. It was shown in Ref. [101] that the model of Beens *et al.* [51] can reproduce the magnetization reversal from the P configuration, but magnetization crosses zero during the remagnetization of the reference layer and it can therefore not explain the experimental measurements of [101]. Igarashi *et al.* [101] therefore concluded that another mechanism has to come into play and suggest a mechanism where a spin current generated by the demagnetization of the free layer is reflected at the Cu/reference layer interface, and upon this reflection, the polarization of the spin current can be rotated. This phenomenon is already well known in the context of spin-transfer torque in noncollinear spin configurations [121]. We propose here to make a simplified model of this mechanism to show that it can explain the qualitative behavior observed in Ref. [101].

The parameters that we use are the same as in the previous section. The only exception is that we take a Curie temperature of 500 K and $J = 0.05$ eV for the free layer. We now need to include spin transport and so we no longer neglect the spin current term of Eq. (13) unless it is explic-

itly stated. We make use of the now well-established result that spin currents are proportional to the spin accumulation when a ferromagnetic layer is in contact with a good spin sink [23,53,64,84]. In our case, considering a given ferromagnetic layer, we assume ballistic spin transport in the Cu spacer layer and this spin sink is the other ferromagnetic layer. For a single ferromagnet/Cu interface, we then assume that the spin current exiting the ferromagnet obeys the following equation [51,84]:

$$\frac{\nabla \cdot \mathbf{J}_s}{\bar{D}} = \frac{\Delta\mu}{\tau_B}, \quad (16)$$

where, following Beens *et al.* [51], we take $\tau_B = 10$ fs for our 10 nm of Cu. Our approach of the simulation of ballistic spin transport is similar to Ref. [51]. We have a single (i.e., depth-independent) d electron magnetization m^{free} and m^{ref} in the free and reference layers, respectively, as well as depth-independent spin accumulations $\Delta\mu^{\text{free}}$ and $\Delta\mu^{\text{ref}}$. The main difference is that we consider that the Cu/reference layer interface has a separate spin accumulation $\Delta\mu^{\text{int}}$. The situation is summarized in Fig. 2. Because we want to simulate reflection at the Cu/reference layer interface, we introduce a parameter $r \in [0, 1]$ that quantifies the amount of spin that is reflected from the interface. r times the spin current coming from the free layer is then transferred to the interface while a fraction $(1 - r)$ is transmitted to the reference layer spin

accumulation. To model the rotation of the spin polarization of the spin current, we then assume that $-\Delta\mu^{\text{int}}/\tau_B$ is transferred from the interface to the free layer (see Fig. 2). This corresponds to a full rotation of the spin polarization. Considering a partial rotation would require, in our simple approach, to introduce an additional parameter which we wish to avoid for this qualitative modeling. In order to conserve angular momentum, however, we need to have a dissipation of the extra $2\Delta\mu^{\text{int}}/\tau_B$ that is generated. Realistically, this dissipation should be independent of the thickness of the spacer layer (which is not the case here since τ_B is given by the spacer thickness divided by the Fermi velocity in the spacer). But, this relationship is enforced by conservation of angular momentum and our assumption of full spin rotation upon reflection. Finally, all the spin current generated by the reference layer is assumed to be completely transmitted to the free layer without transiently stopping by the interface. The complete situation is summarized in Fig. 2 and the corresponding spin current terms entering the spin accumulation dynamics equation (13) of each of the considered ferromagnetic layers are

$$\frac{\nabla \cdot \mathbf{J}_s^{\text{free}}}{\bar{D}} = \frac{\Delta\mu^{\text{free}}}{\tau_B} - \left(-\frac{\Delta\mu^{\text{int}}}{\tau_B} \right) - \frac{\Delta\mu^{\text{ref}}}{\tau_B}, \quad (17a)$$

$$\frac{\nabla \cdot \mathbf{J}_s^{\text{ref}}}{\bar{D}} = \frac{\Delta\mu^{\text{ref}}}{\tau_B} - (1-r) \left(\frac{\Delta\mu^{\text{free}}}{\tau_B} \right), \quad (17b)$$

while the dynamics of the interfacial spin accumulation is

$$\frac{d\Delta\mu^{\text{int}}}{dt} = r \frac{\Delta\mu^{\text{free}}}{\tau_B} - \left(-\frac{\Delta\mu^{\text{int}}}{\tau_B} \right) - 2 \frac{\Delta\mu^{\text{int}}}{\tau_B}, \quad (18)$$

where we wrote all equations in such a way that each term appears in Fig. 2. By setting r to zero, one retrieves ballistic spin transport as it is modeled by Beens *et al.* [51]. Overall, this model generalizes the model of Ref. [94] and so it should also be suitable to reproduce ultrafast magnetization reversal provided that the calculated spin accumulation has the right dynamics and amplitude. For the simulations shown below, we use $r = 0.1$ unless it is stated otherwise. In Appendix B, we compute the angular momentum transfer to the free layer due to the different contributions to the spin current given by Eq. (17a) and discuss its role in the subpicosecond switching of ferromagnetic spin valves.

A. P configuration

In Fig. 3, we show the results of the computed angular momentum dynamics in the spin-valve sample with our model. Figure 3(a) shows the normalized magnetization in the free layer while Fig. 3(b) shows the normalized magnetization of the reference layer. The dynamics is computed for several fluences as shown in Fig. 3(b). We see that the reference layer exhibits the standard UDM plus recovery behavior without any special feature. Consistently with Fig. 1, there is no CSD observable as the normalized magnetization never even reaches 0.2 for these fluences. We note, however, that the spin current coming from the demagnetization of the free layer hinders the demagnetization of the reference layer. This behavior is known to happen in real systems [123]. For the

free layer, we observe only UDM plus recovery at low fluence, magnetization reversal above $F1 \sim 4 \text{ mJ/cm}^2$, and only a transient switching for fluences above $F2 \sim 10 \text{ mJ/cm}^2$. The transient nature of the latter switching is best observed in the inset of Fig. 3(a). This behavior is consistent with the experimental observation of Igarashi *et al.* [101] that the free layer is only permanently reversed for a bounded range of fluences [$F1, F2$] when starting from the P configuration. For fluences which are greater than $F2$ (yet still below the threshold fluence to generate a multidomain state due to a complete quenching of magnetization in the sample), the system remains in the P configuration on a long timescale. A key characteristic of the dynamics observed in [101] is that the free-layer magnetization crosses zero before the reference layer starts to remagnetize. The *s-d* model of Beens *et al.* cannot reproduce this feature [101]. In Fig. 3(c), we plot the magnetization dynamics of both layers for a fluence greater than $F1$ and lesser than $F2$. We also plot the instantaneous equilibrium magnetization of the *d* electrons, for reference. We can see that with our model, the normalized magnetization of the free layer does cross zero before the reference layer starts to remagnetize (this instant is indicated by the vertical dotted line). The time delay between the free-layer magnetization zero crossing and the beginning of the remagnetization of the reference layer increases with fluence. To provide more insight regarding the dynamics of angular momentum and spin transport, we plot the spin accumulations in each layer and at the Cu/reference layer interface in Fig. 3(d). We first note that the spin accumulation inside the free layer has the bipolar shape used in Ref. [94], together with the same order of magnitude, to obtain magnetization reversal of a [Co/Pt] multilayer subjected to a spin current coming from a ferromagnetic GdFeCo. It is known that the spin accumulation needs to be positive to induce the reversal of magnetization. This happens naturally at lower fluences (see Fig. 1(d)) due to remagnetization. For fluences above $F1$, the electronic temperature overcomes the critical temperature of the free layer [see Fig. 4(a)] and, without an external source of angular momentum, CSD will appear [94]. From Eq. (13), it follows that the spin accumulation will be negative at all times (the terms containing the instantaneous equilibrium magnetization can lead to a positive spin accumulation when the light source term is not zero, but this effect is negligible). This ensures that a ferromagnetic layer cannot reverse its magnetization because of the spin accumulation it generates, in normal circumstances. The positive spin accumulation peak of the free layer in Fig. 3(d) is due to the spin current reflection mechanism. One can see that after a certain delay due to the ballistic spin transport, a spin accumulation starts reaching the Cu/reference layer interface. Because the corresponding angular momentum is reversed upon being reflected back to the free layer, this leads to an increase of the spin accumulation of the free layer which eventually becomes positive. Once the free-layer spin accumulation becomes positive, the spin accumulation at the interface starts to decrease. The spin accumulation of the reference layer also has this bipolar structure because (i) the reference layer remagnetizes and (ii) the ballistic spin transport (17b) tends to bring the spin accumulation curve of the reference layer closer to the one of the free layer (and vice versa).

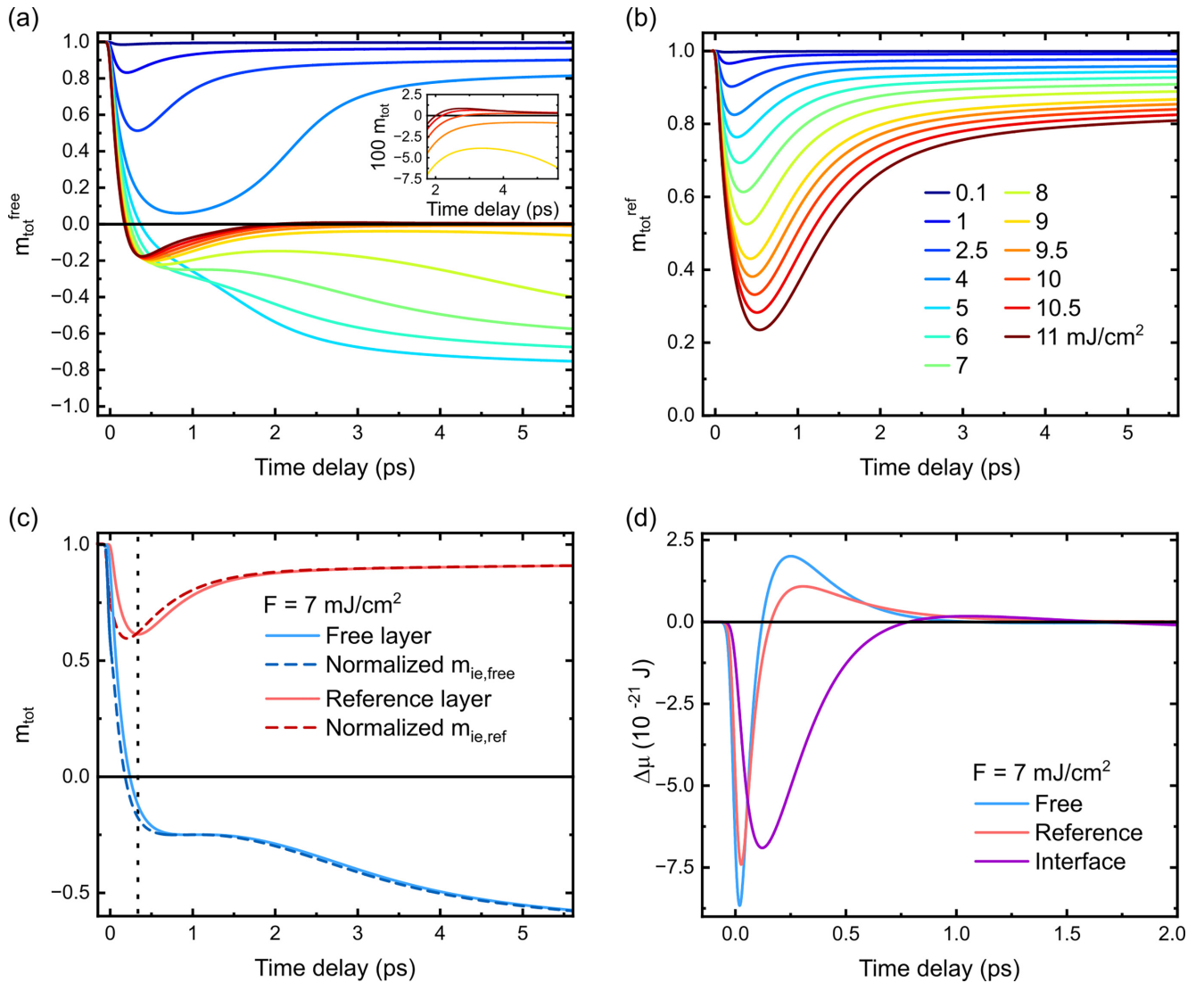


FIG. 3. Normalized magnetization dynamics of the spin-valve sample where the dynamics of the free layer is shown in (a) and the one of the reference layer is shown in (b), for various fluences as indicated in (b). The inset of (a) shows a zoom between 2 and 5 ps where the normalized magnetization has been scaled by a factor of 100. (c) Shows the same data as (a) and (b) for a fluence of 7 mJ/cm² together with the normalized instantaneous equilibrium d electron magnetization of each layer; the vertical dotted line indicates the time instant where the magnetization of the reference layer starts to recover. (d) Shows the calculated spin accumulation dynamics in each layer as well as at the Cu/reference layer interface.

We now look at some other effects predicted by our model in this spin valve. First, we look at the electron and phonon temperature dynamics in each ferromagnetic layer. This is shown in Figs. 4(a) and 4(b) for the free and reference layers, respectively. A standard dynamics, as obtained from the two-temperature model, is obtained at first glance. Upon closer inspection, we can see, however, some bumps or additional peaks in the electron temperature dynamics for certain fluences. We adjusted the scale so as to make this effect obvious for the free layer, therefore cutting off the first peak of the dynamics which does not show any interesting feature. The deviation from the standard two-temperature model dynamics is especially large when no reversal of magnetization is obtained. These extra features, such as the peak around 2.5 ps in the free layer for 4 mJ/cm², is due to the increase of magnetization (in absolute value) via the magnetization-dependent

term in Eq. (6a). Although these peaks may be overestimated due to the fact that the mean field model tends to overestimate the speed of remagnetization around $m = 0$, we still observe a sizable effect of the transfer of energy from d to s electrons in the reference layer while such effect did not exist for a single layer with parameters identical to that reference layer (Sec. III). We therefore conclude that an external source of angular momentum, via a spin current, can heat up electrons in a way that should be observable experimentally.

Now, we look at the role of the dynamic exchange splitting, spin currents, and d to s energy transfer on the magnetization dynamics of spin valves. To do so, we plotted in Fig. 5 the magnetization dynamics of the free layer for two fluences and different models. First, we can neglect the role of dynamic exchange splitting (“ $J = 0$ ”). For the highest fluence, where magnetization does not stay around zero, a very little

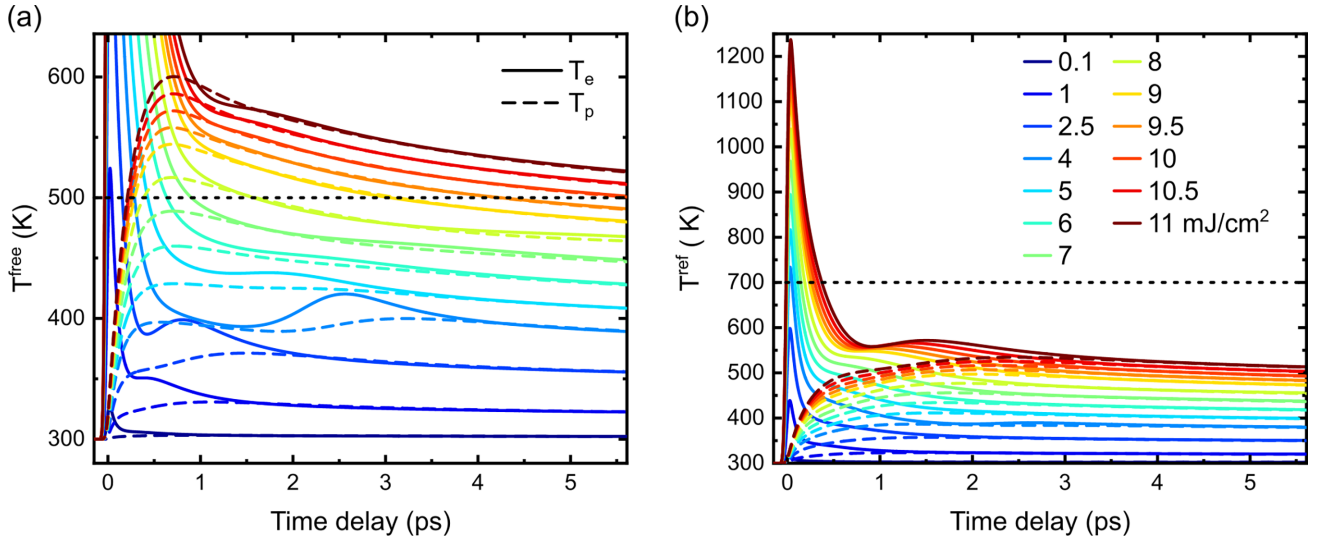


FIG. 4. Temperature dynamics of electrons (solid lines) and phonons (dashed lines) for the (a) free and (b) reference layers. The dynamics is calculated for various fluences as indicated in (b). The Curie temperature of each layer is indicated in each case by the horizontal dotted line.

difference is obtained. On the other hand, for the lower fluence, we can see a significant difference which results either in a reversal or not. Including the dynamic exchange splitting will not qualitatively change the magnetization dynamics but it can have sizable quantitative effects and so should also be considered in more realistic models. Then, we can also neglect the d to s electron energy transfer (“ $\dot{E}_{es} = 0$ ”). This can lead to large effects but the reason is, just as for the single-layer case, that it will change the maximum electron temperature. We can also block all spin transport which prevents any magnetization reversal even for high fluences (not shown). We can see that blocking this spin current also has a large effect on the magnetization dynamics. Even though our value of the reflection parameter r is quite arbitrary, this

should not come as a surprise as it was observed experimentally that spin heating (i.e., a decrease of magnetization solely due to an external source of angular momentum) can lead to a change of magnetization of up to 50% [94]. Finally, we compare these results with the calculations obtained with the model of Beens *et al.* [51]. This model can also lead to magnetization reversal of the free layer but at higher fluence and the zero crossing happens for larger time delays [101]. Because temperatures are higher for higher fluences, the maximum reachable normalized magnetization is smaller and the effect of the spin current in Beens *et al.* model is smaller, at least for our choice of parameters. Overall, Figs. 3 and 5 illustrate the rich varieties of dynamics which can be expected in spin valves compared to single layers where there is only

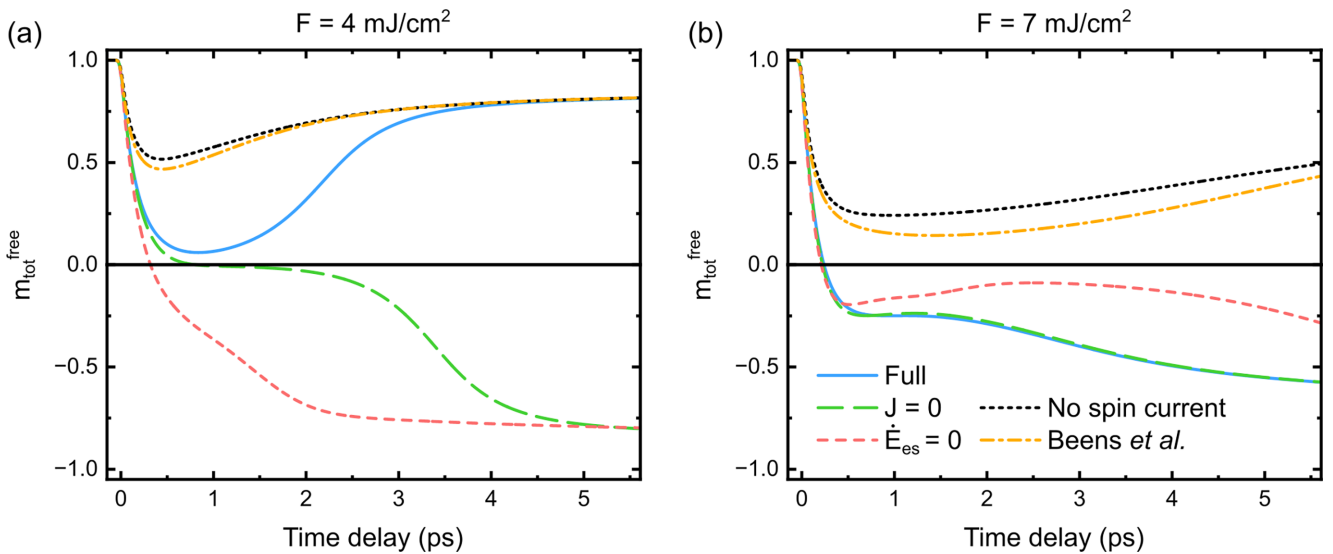


FIG. 5. Normalized magnetization dynamics of the free layer computed for (a) 4 and (b) 7 mJ/cm² for different models. “Full” corresponds to the full equation (14a) with $J = 0.1$ (reference layer) and 0.05 (free layer) eV and $\alpha = 1$; “ $J = 0$ ” is obtained by setting $J = 0$ eV for both ferromagnetic layers; “ $\dot{E}_{es} = 0$ ” is obtained by neglecting the magnetization-dependent term in Eq. (6a); “No spin current” is obtained by neglecting all spin transport; “Beens *et al.*” is obtained by setting $r = 0$ and $J = 0$.

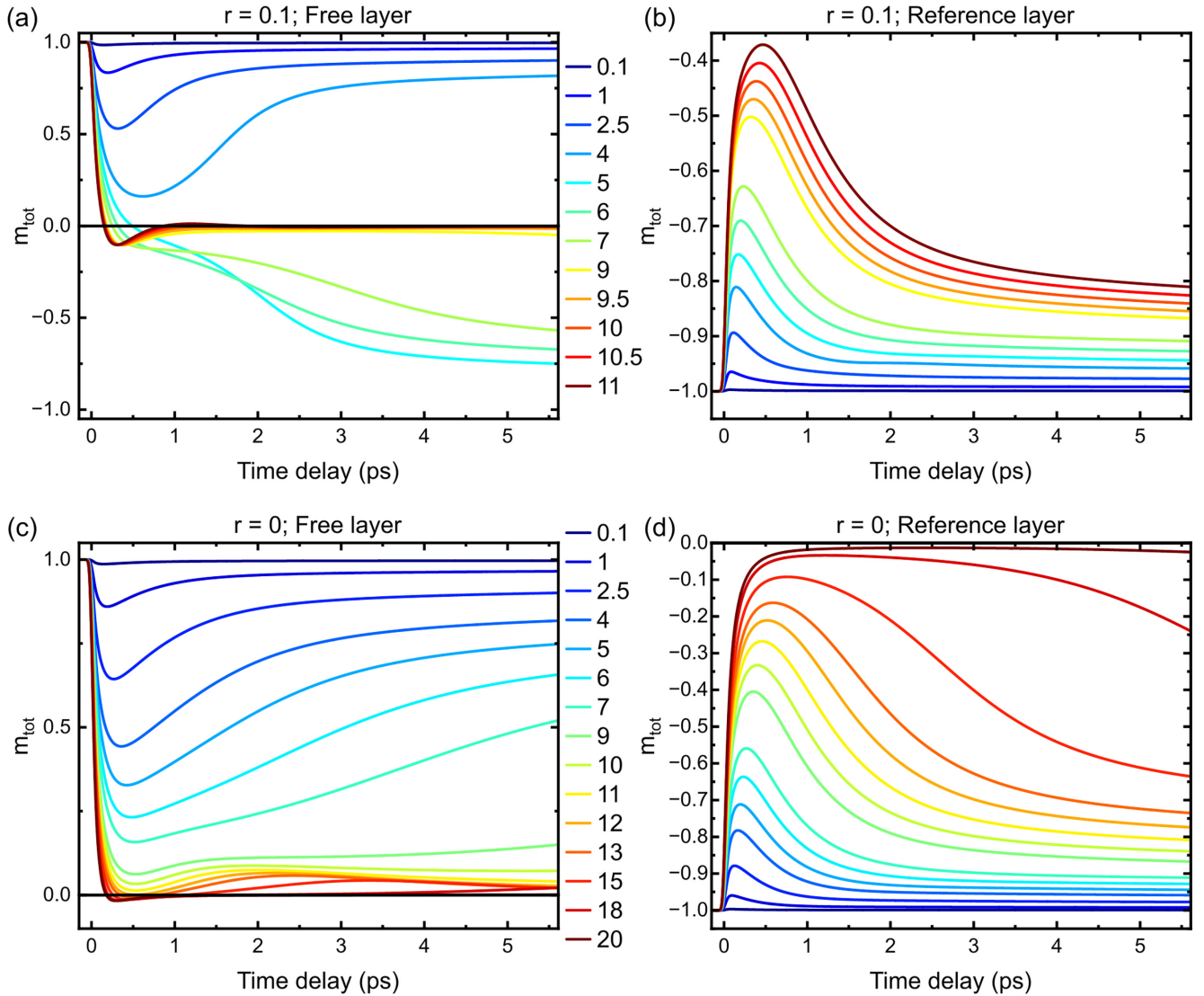


FIG. 6. Normalized magnetization dynamics for the (a), (c) free and (b), (d) reference layers. In (a) and (b), we use $r = 0.1$ while in (c) and (d) we use $r = 0$. For (a) and (b), the considered fluences (in mJ/cm^2) are indicated on the right of plot (a) while for (c) and (d) they are indicated on the right of plot (c).

demagnetization followed by remagnetization. This diversity and its strong fluence and parameter dependence should be kept in mind when studying the ultrafast magnetization dynamics of spin-valve heterostructures. Such diversity of behaviors has already been observed experimentally [92,99].

B. AP configuration

To finish this section, we calculate the dynamics of the spin valve when it is initially prepared in an AP configuration. In practice, we run exactly the same simulations except that out of the two stable equilibrium magnetizations of the reference layer, we select the solution with a negative sign instead of the positive one. We always keep the positive solution for the free layer. We assume that the reflection mechanism is identical to the P case. In particular, the spin polarization is rotated the same way independently of the magnetic configuration of the reference layer, consistently with the model introduced above. The results are shown in Figs. 6(a)

and 6(b). Apart from the obvious sign change for the reference layer, the results are almost identical to the simulations of the P case. A difference of interest, consistent with experiments [101], is that it is harder to switch the free layer from the AP configuration compared to the P configuration, although the effect is much smaller than in the experiments (check the slightly reduced quenching of magnetization for a fluence of 4 mJ/cm^2 in both cases). However, in the experiments, the transient reversal of the free layer from the P configuration starts happening for fluences F_2 almost identical to the threshold fluence F_1' required to observe a reversal of the free layer from the AP configuration, i.e., $F_1' \sim F_2$. This is not the case in our simulations where $F_1' \gtrsim 4 \text{ mJ/cm}^2$ while $F_2 \sim 10 \text{ mJ/cm}^2$. We note that Igarashi *et al.* [101] do not consider this reflection mechanism for the AP configuration. We thus perform simulations for $r = 0$ in Fig. 6(c) and 6(d). However, no permanent reversal of the free-layer magnetization is observed. Although a transient reversal is observed starting from fluences around 12 mJ/cm^2 , the remagnetization of the

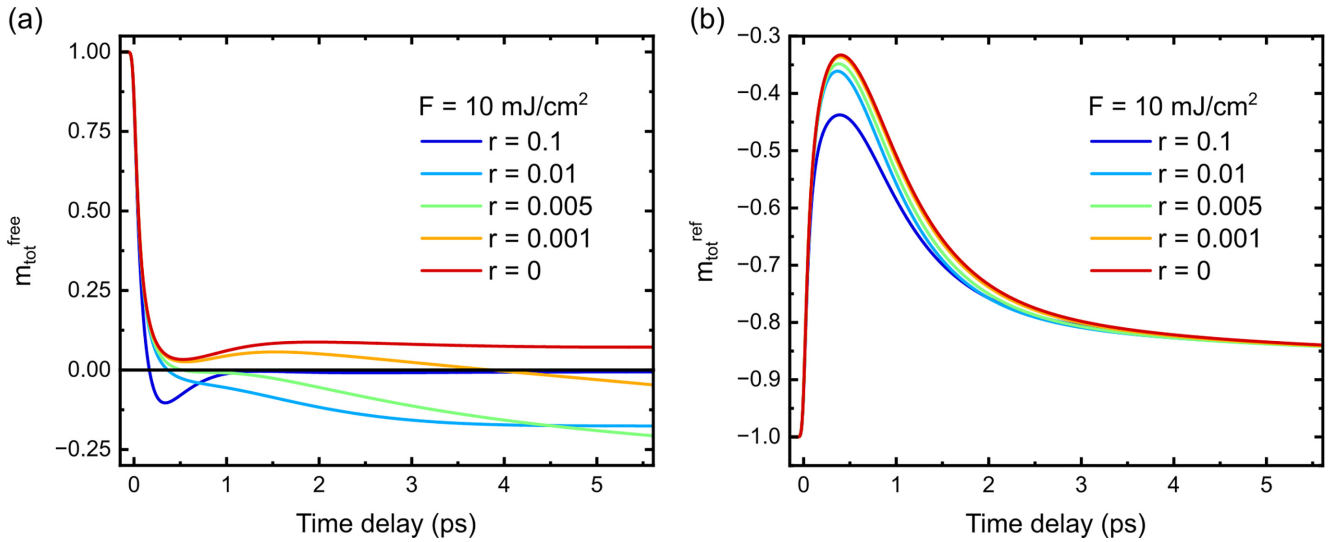


FIG. 7. Normalized magnetization dynamics of the (a) free and (b) reference layers in the AP configuration and for different values of r as indicated.

reference layer prevents the reversal from being permanent. Even at much higher fluences, when the remagnetization of the reference layer is greatly hindered due to CSD, a permanent reversal is still not possible. This is because the magnetization of the free layer is also further reduced, which makes it even more sensitive to spin currents. In real systems, a multidomain state would be generated at such high fluences. The transient nature of the reversal at these higher fluences could also be due to the overestimation of remagnetization by mean field models.

It could also be possible that a reflection mechanism is still present in the AP configuration, even though it would be different, for reasons we do not explain, from the reflection mechanism when one starts from the P configuration. This is supported by some experimental measurements of Igarashi *et al.* [101] where a reversal of the free layer from an AP configuration is still observed for a copper spacer with a thickness of 40 nm. In this case, only a small amount of light can reach the reference layer which also supports a contribution of the spin current reflection mechanism. In Fig. 7, we compute the magnetization dynamics of both layers for a fluence around $F/2$ and for different values of r . The magnetization dynamics of the reference layer remains qualitatively the same for the considered reflection parameters. The one of the free layer is, however, significantly modified. As a general trend, we see that lowering the value of the r parameter slows down the reversal dynamics, i.e., the normalized magnetization crosses zero for larger time delays. It is also interesting to note that in all cases, the temperature dynamics are almost identical (± 2 K) even though the d to s electron energy transfer is different for different values of r . This means that one cannot in general conclude that a magnetic subsystem is at equilibrium from the fact that its magnetization almost no longer changes (as it is observed for instance in Fig. 7(a) for $r = 0, 0.01, \text{ and } 0.1$). It is possible that an out-of-equilibrium situation is sustained due to a spin current emitted by another layer where the dynamics is still not over (here the reference layer; see Fig. 7(b)).

We conclude this section by highlighting that our spin current reflection mechanism is probably oversimplified. We note, however, that our approach, based on parameters with reasonable values, shows that this mechanism, if it exists, generates spin accumulations with a reasonable order of magnitude and triggers a magnetization dynamics with a realistic speed.

V. CONCLUSION

In this work, we presented an extension of the s - d model based on Refs. [22,51,102,103] which includes a dynamic exchange splitting (and equilibrium spin polarization of the s band), energy transfer from d to s electrons [67,111], as well as a proposed spin current reflection mechanism [101]. This model leads to qualitatively (and also mostly quantitatively) identical results in single ferromagnetic layer systems compared to the case where all these additional effects are neglected. In the case where there is an external or nonlocal source of angular momentum such as in spin valves, we showed that these effects can drastically change the observed magnetization dynamics. In particular, we could reproduce the magnetization reversal of the free layer of a ferromagnetic spin valve which cannot be qualitatively reproduced by previous models. We also predict that the electronic temperature dynamics may be strongly affected, for instance, in such spin valves, when a ferromagnetic material is subjected to an external source of angular momentum.

The advantage of our model is that it is not computationally expensive but, as pointed out in this paper, it lacks quantitative predictive power. In particular, the mechanism for the reflection of the spin current is still unclear. It is also not clear whether the s - d model is well suited for such simulations as it does not contain magnons which are believed to play a fundamental role at the ferromagnetic or paramagnetic transition [124]. Transverse excitations, however, are included in this mean field model, but the fast recovery of magnetization (we mean even in the absence of an external source of angular

momentum), once it has almost been quenched, compared to experiments [94] or atomistic simulations [59], seems to indicate that at least the mean field approximation needs to be lifted in order to make more quantitative predictions. Still, our model is attractive for its simplicity and its capability to explain the diversity of ultrafast magnetization dynamics behaviors.

A quantitative agreement could also perhaps be obtained by following the approach of Ref. [67] by using, for instance, temperature-dependent parameters, but considering the number of parameters required in such simulations, it is not yet clear whether these calculations can have any quantitative predicting power for such complex systems. An alternative route, largely unexplored in the field of ultrafast magnetization dynamics, would be to treat the electron-magnon problem within the framework of the Fermi-liquid theory [125].

ACKNOWLEDGMENTS

The author thanks J. Gorchon, G. Malinowski, J. Igarashi, G. Nava Antonio, C. Ciccarelli, P. Scheid, and S. Mangin for valuable discussions. This work is supported by the Grant No. ANR-20-CE09-0013 UFO, by the Institute Carnot ICEEL for the project ‘‘CAPMAT’’ and FASTNESS, by the R egion Grand Est, by the Metropole Grand Nancy, for the Chaire PLUS by the impact Project No. LUE-N4S, part of the French PIA project ‘‘Lorraine Universit e d’Excellence’’ Reference No. ANR-15-IDEX-04-LUE, by the ‘‘FEDERFSE Lorraine et Massif Vosges 2014-2020,’’ a European Union Program, by the European Union’s Horizon 2020 research and innovation program COMRAD under the Marie Skłodowska-Curie Grant Agreement No. 861300. This paper is based upon work from COST Action CA17123 MAGNETOFON, supported by COST (European Cooperation in Science and Technology). We also acknowledge funding by the German Research Foundation (DFG) through the collaborative research center SFB TRR 227 ‘‘Ultrafast spin dynamics’’ (Project ID 328545488, Project No. B02) and the European Union H2020 program through the FET project SKYTOP Grant No. 824123.

APPENDIX A: DERIVATION OF EQ. (8)

In this Appendix, we provide a derivation of Eq. (8). This equation was first given in Ref. [22], to the best of our knowledge, but its derivation and validity was not discussed. This derivation is useful to establish the limitations of the equations given in this work as well as to show the need for a more realistic description of the materials densities of state. We need to calculate the s electron spin polarization

$$s^z = \frac{N_\uparrow - N_\downarrow}{2N} \quad (\text{A1})$$

with $N = N_\uparrow + N_\downarrow$ the total number of s electrons and N_σ is the number of electrons with spin σ . Note that when all s electrons have an up spin, $s^z = \frac{1}{2}$ and so this definition of the spin polarization is consistent with the equations of the main text. The spin-dependent electronic numbers are obtained from

$$N_\sigma = \int D_\sigma(E) f(E; T_e, \mu_\sigma) dE \quad (\text{A2})$$

with f the Fermi-Dirac distribution function. However, Eq. (8) does not depend on the electronic temperature explicitly. Thus, we first need to approximate the Fermi-Dirac functions by step functions. This means that the thermal energy should be much smaller than the width of the s band: $k_B T_e \ll \mu_\sigma - E_\sigma^0$. Then

$$N_\sigma = \int_{E_\sigma^0}^{\mu_\sigma} D_\sigma(E - E_\sigma^0) dE = \mathcal{D}_\sigma(\mu_\sigma - E_\sigma^0) - \mathcal{D}_\sigma(0), \quad (\text{A3})$$

where we shifted the functions representing the densities of state for convenience and we also assumed that these functions are continuous such that they all have an antiderivative \mathcal{D}_σ . We now perform three consecutive first-order Taylor expansions of $\mathcal{D}_\sigma(\mu_\sigma - E_\sigma^0)$, assuming that $\Delta\mu$, $\mu - \mu_{ie}$, and $E_\sigma^0 - E_{\sigma,ie}^0$ are small compared to $\mu_\sigma - E_\sigma^0$. $\mu_\sigma = \mu + \sigma \Delta\mu/2$ and the ‘‘ie’’ subscript refers to instantaneous equilibrium value as for the spin polarization s_{ie}^z . We obtain

$$\begin{aligned} N_\sigma &\simeq \mathcal{D}_\sigma(\mu_{\sigma,ie} - E_{\sigma,ie}^0) - \mathcal{D}_\sigma(0) \\ &+ \sigma \frac{\Delta\mu}{2} \mathcal{D}_\sigma(\mu - E_\sigma^0) \\ &+ (\mu - \mu_{ie}) \mathcal{D}_\sigma(\mu_{ie} - E_\sigma^0) \\ &- (E_\sigma^0 - E_{\sigma,ie}^0) \mathcal{D}_\sigma(\mu_{ie} - E_{\sigma,ie}^0). \end{aligned} \quad (\text{A4})$$

To the same level of approximation, all the density-of-states factors should be taken equal, and after shifting back the function representing the densities of state, one has

$$N_\sigma \simeq N_{\sigma,ie} + D_\sigma(\varepsilon_F) \left[(\mu - \mu_{ie}) + \sigma \frac{\Delta\mu}{2} - (E_\sigma^0 - E_{\sigma,ie}^0) \right]. \quad (\text{A5})$$

Using the fact that the total number of s electrons does not change $N = N_{ie} = N_{\uparrow,ie} + N_{\downarrow,ie}$, one obtains

$$\begin{aligned} \mu - \mu_{ie} &= - \frac{D_\uparrow(\varepsilon_F) - D_\downarrow(\varepsilon_F)}{D_\uparrow(\varepsilon_F) + D_\downarrow(\varepsilon_F)} \frac{\Delta\mu}{2} \\ &+ \frac{D_\uparrow(\varepsilon_F)}{D_\uparrow(\varepsilon_F) + D_\downarrow(\varepsilon_F)} (E_\uparrow^0 - E_{\uparrow,ie}^0) \\ &+ \frac{D_\downarrow(\varepsilon_F)}{D_\uparrow(\varepsilon_F) + D_\downarrow(\varepsilon_F)} (E_\downarrow^0 - E_{\downarrow,ie}^0). \end{aligned} \quad (\text{A6})$$

Equation (8) is readily obtained by combining Eqs. (A1), (A5), and (A6).

Now $(E_\sigma^0 - E_{\sigma,ie}^0) \sim J$ and Eq. (A3) implies that $\mu_\sigma - E_\sigma^0 \sim 1/\bar{D}$. So to be consistent, our theory should be such that $\Delta\mu$, J , and $k_B T_e$ are much smaller than $1/\bar{D}$. We have used $J = 0.1/\bar{D}$ and for the highest studied fluences, we have $k_B T_e \simeq 0.2/\bar{D}$ and $\Delta\mu \simeq 0.1/\bar{D}$. However, this does not invalidate the qualitative nature of our results since we obtain similar results for $J = 0$ and the magnetization switching in the spin valve appears at relatively low fluences. Nevertheless, we note that using larger values of J (in combination with fluences comparable to the ones used in this work) leads to large divergences in the spin accumulation because of the factor $1/[1 - JS\eta(t)/[2k_B T_e(t)]]$ in Eq. (14a). No such behavior was observed for the results presented in this work.

APPENDIX B: SPIN ANGULAR MOMENTUM OF S ELECTRONS

In this Appendix, we discuss the amount of spin angular momentum (meaning average of the z components of spin operators, as in the main text) received and stored in the s electrons bath in our model during the magnetization reversal of the free layer for the spin valve in the P configuration. The purpose of this section is also to show that the dynamics observed in the main text is not due to an unphysically large amount of angular momentum existing in the free layer. Contrary to the main text, we consider non-normalized quantities, and angular momentum instead of magnetization (hence the occurrence of a minus sign in the results we show). We focus on the case where the externally applied fluence is 7 mJ/cm^2 . Similarly to the main text, we consider angular momentum in units of \hbar and per atom.

The black lines in Fig. 8(a) display the same results as Fig. 3(c) but in terms of the total spin angular momentum instead of normalized magnetization. The colored lines of the same figure show the individual contributions of s and d electrons in each layer. Because $\chi = 1$, both contributions in the s and d electrons are initially identical. The initial amount of spin angular momentum is different in each layer because both layers have different Curie temperatures. One observes that the dynamics of s and d electrons is almost identical at all times. This is consistent with the fact that the generated out-of-equilibrium spin angular momentum in s electrons is quite small for the value of \bar{D} that we used, as can be seen (for s electrons close to the Fermi level) in Fig. 9. Looking at the dynamics around zero time delay (see the inset of Fig. 8(a)) one can see that the spin angular momentum in s electrons of the reference layer slightly overcomes the value $\frac{1}{2}$ to reach around 0.504. This unphysical result comes from the fact that when $\chi = 1$, $\mu_\sigma - E_\sigma^0$ becomes a small quantity (different from zero at nonzero temperatures) in the spin minority channel and so the validity of Eq. (8) is more doubtful. Thus, in Fig. 8(b), we reproduce the same calculations for $\chi = 0.1$. We see that the results are qualitatively the same except that the amount of angular momentum in the s electrons is about 10 times smaller than in the d electrons during the entire dynamics. We conclude that the parameter χ plays a minor role in the qualitative dynamics of spin valves. The main role of this parameter is to slightly change the efficiency of the “ $-dM/dt$ ” mechanism as Eq. (14a) shows as well as changing the equilibrium spin polarization of conduction electrons. We also show the results obtained with a smaller reflection coefficient $r = 0.01$ while keeping $\chi = 1$ in Fig. 8(e). In this case, the magnetization zero crossing happens later, otherwise, the same comments as for Fig. 8(a) apply. In particular, roughly the same amount of angular momentum is stored in s and d electrons whether $r = 0.1$ or 0.01 . This also shows that the angular momentum stored in conduction electrons is mostly driven by its equilibrium value since Eq. (9) is approximately verified at all times, i.e., the deviation from Eq. (9) is small compared to the room-temperature equilibrium angular momentum.

One may wonder what is the total amount of angular momentum received by the free layer, after irradiation with a laser pulse and due to spin currents, which can lead to

magnetization reversal. More specifically, we want to calculate the amount of angular momentum that has entered or left the conduction band of the free layer at a specific instant due to spin currents. According to Eq. (17a), these quantities depend on

$$\Delta s_{j_s}^{z,\text{free}}(t) = \frac{\bar{D}}{\tau_B} \int_{-\infty}^t -\Delta \mu^{\text{free}}(t') dt', \quad (\text{B1a})$$

$$\Delta s_{j_s}^{z,\text{ref}}(t) = \frac{\bar{D}}{\tau_B} \int_{-\infty}^t \Delta \mu^{\text{ref}}(t') dt', \quad (\text{B1b})$$

$$\Delta s_{j_s}^{z,\text{int}}(t) = \frac{\bar{D}}{\tau_B} \int_{-\infty}^t -\Delta \mu^{\text{int}}(t') dt'. \quad (\text{B1c})$$

These three quantities are plotted on the right panels of Fig. 8. In general, a positive value of $\Delta s_{j_s}^{z,i}(t)$, with i being free, ref, or int, corresponds to a total spin angular momentum that has left the free layer at t which is negative or, equivalently, a total spin angular momentum that has entered the free layer which is positive. We adopt the picture, consistent with Fig. 2, where $\Delta s_{j_s}^{z,\text{free}}$ always refers to angular momentum that leaves the free layer while $\Delta s_{j_s}^{z,\text{ref}}$ and $\Delta s_{j_s}^{z,\text{int}}$ always refer to angular momentum that enters the free layer. Then, initially, the free layer loses negative angular momentum due to the spin current driven by the free layer (i.e., spin injection in the Cu spacer layer) and gains negative angular momentum due to the spin current coming from the reference layer. The spin current coming from the reflection mechanism provides positive angular momentum and a clear delay is observable compared to the other two terms, which is due to the fact that this spin current travels through the Cu layer twice. The total angular momentum received by the free layer $\Delta s_{j_s}^{z,\text{ref+int}} = \Delta s_{j_s}^{z,\text{ref}} + \Delta s_{j_s}^{z,\text{int}}$ is plotted in black. We can see that it is first dominated by the spin current coming from the reference layer and is then largely dominated by the reflection mechanism. One can see that the values of $\Delta s_{j_s}^{z,\text{ref+int}}$ can become larger than $\frac{1}{2}$. However, two important comments should be made. First, a quantity more relevant for magnetization reversal of the free layer (compared to the values of $\Delta s_{j_s}^{z,\text{ref+int}}$ at long time delays) is the total spin angular momentum received by the free layer before the magnetization of this layer crosses zero. This quantity is seen in Fig. 8 to be always smaller than $\frac{1}{2}$. Second, the dynamics is self-consistent which means that angular momentum received by the free layer can later leave the free layer again before coming back, i.e., the same angular momentum can be accounted for several times. Interestingly, we see that for the lower value of χ , the values of $\Delta s_{j_s}^{z,i}$ are about half as large but with a similar dynamics. For a lower value of the reflection coefficient, the amplitude of each term is larger but their dynamics is slower. In this case, the reflection mechanism is less efficient so $\Delta s_{j_s}^{z,\text{int}}$ takes more time to build up and the standard ballistic spin transport as described in Ref. [51] dominates leading to larger values of $\Delta s_{j_s}^{z,\text{free}}$ and $\Delta s_{j_s}^{z,\text{ref}}$. The fact that the latter two terms reach absolute values larger than $\frac{1}{2}$ within a few hundreds of femtoseconds is a consequence of the aforementioned fact that the same angular momentum can be accounted for several times. Even more interesting in this case with $r = 0.01$, one sees that the total angular momentum received by the free layer before

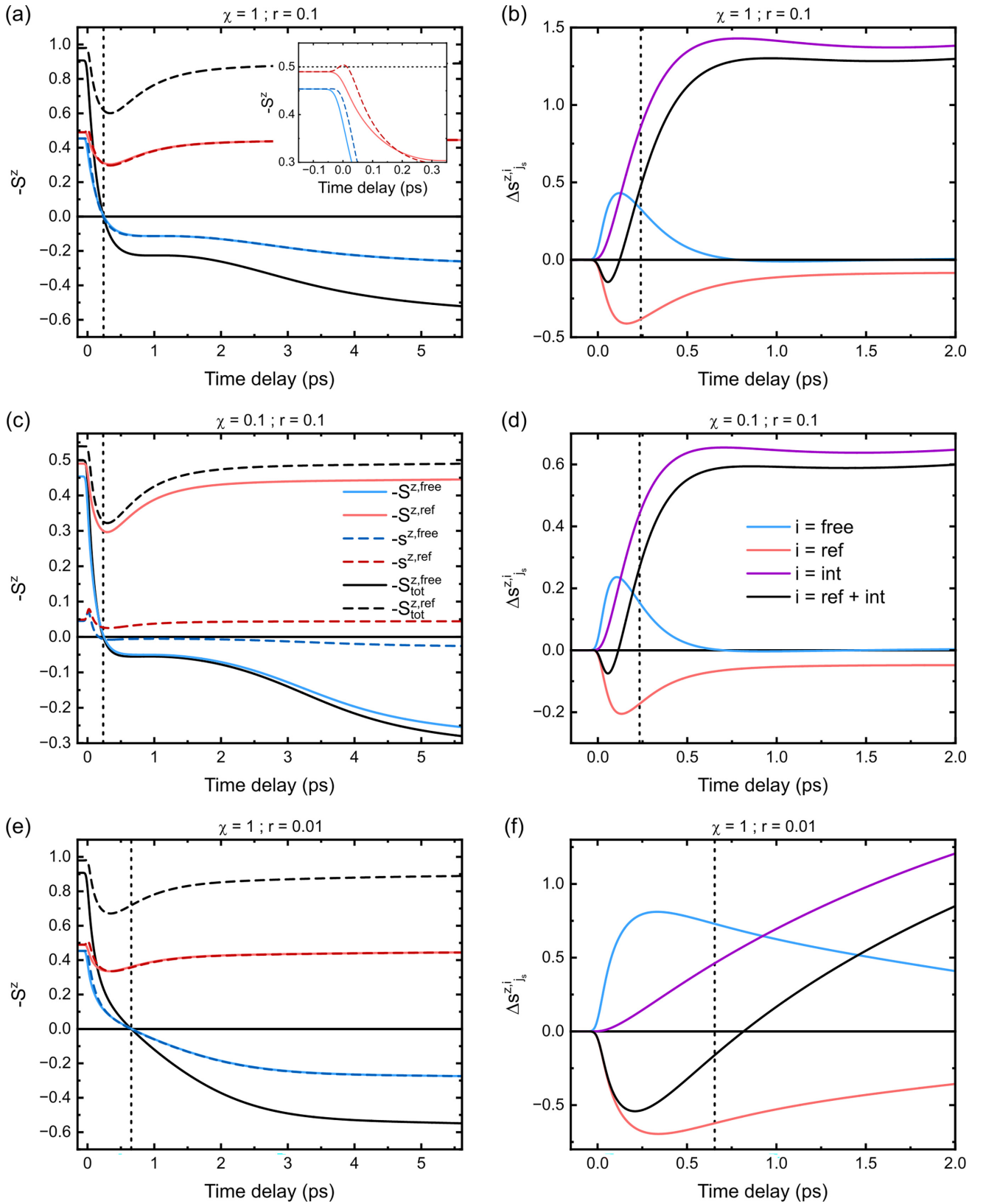


FIG. 8. (a), (c), (e) Spin angular momentum dynamics of the spin-valve structure in the P configuration for three different choices of the pair of parameters χ and r as indicated at the top of each panel. Spin angular momenta in the free and reference layers for the s (s^z), the d electrons (S^z), and the sum of both (S_{tot}^z) are displayed as shown in the legend in (c). (b), (d), (f) Show the total change of spin angular momentum in the free layer due to spin currents $\Delta S_{js}^{z,i}$, as defined in the text, for the corresponding choices of parameters. The vertical dashed lines indicate the time delay at which the total spin angular of the free layer crosses zero. The inset in (a) is a zoom around zero time delay with the horizontal dashed line indicating a spin polarization of $\frac{1}{2}$. The fluence is 7 mJ/cm^2 .

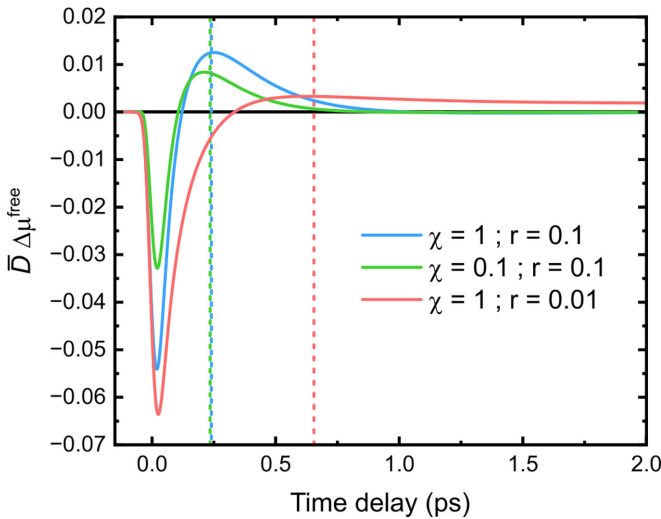


FIG. 9. Contribution to the out-of-equilibrium spin angular momentum in the s electrons $\bar{D}\Delta\mu^{\text{free}}$ for electrons close to the Fermi level, in the free layer. The dynamics is shown for the same three sets of parameters as in Fig. 8. The vertical dashed lines indicate the time delay at which the total spin angular of the free layer crosses zero, for each set of parameters as indicated in the legend.

its magnetization crosses zero is negative. We thus conclude that one should not simply look at the total amount of angular

momentum received (and emitted) by the free layer, in general because this angular momentum may not be transferred to the d electrons but emitted as a spin current or dissipated in the lattice. We note that the total angular momentum received by the d electrons can be directly read from the left panels of Fig. 8.

A more relevant quantity to understand the angular momentum transport leading to magnetization reversal is the angular momentum stored in conduction electrons close to the Fermi level in the free layer, i.e., $\bar{D}\Delta\mu^{\text{free}}$. We plot this quantity for the three sets of parameters considered in this Appendix in Fig. 9. $\bar{D}\Delta\mu^{\text{free}}(t)$ accounts for the fact that some angular momentum received by the free layer may be transferred to the lattice or back to the Cu spacer instead of the d electrons, as given by Eq. (13). This quantity gives the total amount of spin angular momentum that has been generated in the conduction electrons up to an instant t and that can be exchanged with the d electrons. Before the reversal, indicated by the dashed vertical lines in Fig. 9, we see that this quantity reaches around 0.013 for the same set of parameters as in the main text, 0.008 for $\chi = 0.1$ and 0.003 for $r = 0.01$. Note that without the spin current terms in Eq. (13), $\bar{D}\Delta\mu^{\text{free}}$ can never be positive, as discussed in the main text. Thus, we argue that a total (meaning taking into account what enters and what leaves) angular momentum transferred to the conduction electrons close to the Fermi level of only a few percent of the room-temperature equilibrium value (0.45 for $\chi = 1$) is sufficient to trigger magnetization reversal of the free layer.

- [1] M. B. Agranat, S. I. Ashitkov, A. B. Granovskii, and G. I. Rukman, Interaction of picosecond laser pulses with the electron, spin, and phonon subsystems of nickel, *Zh. Eksp. Teor. Fiz* **86**, 1376 (1984) [*Sov. Phys. JETP* **59**, 804 (1984)].
- [2] A. Vaterlaus, T. Beutler, and F. Meier, Spin-lattice Relaxation Time of Ferromagnetic Gadolinium Determined with Time-Resolved Spin-Polarized Photoemission, *Phys. Rev. Lett.* **67**, 3314 (1991).
- [3] E. Beaupaire, J.-C. Merle, A. Daunois, and J.-Y. Bigot, Ultrafast Spin Dynamics in Ferromagnetic Nickel, *Phys. Rev. Lett.* **76**, 4250 (1996).
- [4] A. Scholl, L. Baumgarten, R. Jacquemin, and W. Eberhardt, Ultrafast Spin Dynamics of Ferromagnetic Thin Films Observed by fs Spin-Resolved Two-Photon Photoemission, *Phys. Rev. Lett.* **79**, 5146 (1997).
- [5] J. Hohlfeld, E. Matthias, R. Knorren, and K. H. Bennemann, Nonequilibrium Magnetization Dynamics of Nickel, *Phys. Rev. Lett.* **78**, 4861 (1997).
- [6] U. Conrad, J. Güdde, V. Jähne, and E. Matthias, Ultrafast electron and magnetization dynamics of thin Ni and Co films on Cu(001) observed by time-resolved SHG, *Appl. Phys. B* **68**, 511 (1999).
- [7] P. Scheid, Q. Remy, S. Lebègue, G. Malinowski, and S. Mangin, Light induced ultrafast magnetization dynamics in metallic compounds, *J. Magn. Magn. Mater.* **560**, 169596 (2022).
- [8] M. Battiato, K. Carva, and P. M. Oppeneer, Superdiffusive Spin Transport as a Mechanism of Ultrafast Demagnetization, *Phys. Rev. Lett.* **105**, 027203 (2010).
- [9] M. Battiato, K. Carva, and P. M. Oppeneer, Theory of laser-induced ultrafast superdiffusive spin transport in layered heterostructures, *Phys. Rev. B* **86**, 024404 (2012).
- [10] A. J. Schellekens, W. Verhoeven, T. N. Vader, and B. Koopmans, Investigating the contribution of superdiffusive transport to ultrafast demagnetization of ferromagnetic thin films, *Appl. Phys. Lett.* **102**, 252408 (2013).
- [11] C. E. Graves, A. H. Reid, T. Wang, B. Wu, S. de Jong, K. Vahaplar, I. Radu, D. P. Bernstein, M. Messerschmidt, L. Müller, R. Coffee, M. Bionta, S. W. Epp, R. Hartmann, N. Kimmel, G. Hauser, A. Hartmann, P. Holl, H. Gorke, J. H. Mentink *et al.*, Nanoscale spin reversal by non-local angular momentum transfer following ultrafast laser excitation in ferrimagnetic GdFeCo, *Nat. Mater.* **12**, 293 (2013).
- [12] J. Wieczorek, A. Eschenlohr, B. Weidtmann, M. Rösner, N. Bergard, A. Tarasevitch, T. O. Wehling, and U. Bovensiepen, Separation of ultrafast spin currents and spin-flip scattering in Co/Cu(001) driven by femtosecond laser excitation employing the complex magneto-optical Kerr effect, *Phys. Rev. B* **92**, 174410 (2015).
- [13] N. Moisan, G. Malinowski, J. Mauchain, M. Hehn, B. Vodungbo, J. Lüning, S. Mangin, E. E. Fullerton, and A. Thiaville, Investigating the role of superdiffusive currents in laser induced demagnetization of ferromagnets with nanoscale magnetic domains, *Sci. Rep.* **4**, 4658 (2015).
- [14] J. K. Dewhurst, P. Elliott, S. Shallcross, E. K. U. Gross, and S. Sharma, Laser-induced intersite spin transfer, *Nano Lett.* **18**, 1842 (2018).

- [15] B. Koopmans, G. Malinowski, F. D. Longa, D. Steiauf, M. Fähnle, T. Roth, M. Cinchetti, and M. Aeschlimann, Explaining the paradoxical diversity of ultrafast laser-induced demagnetization, *Nat. Mater.* **9**, 259 (2010).
- [16] K. Carva, M. Battiato, and P. M. Oppeneer, *Ab Initio* Investigation of the Elliott-Yafet Electron-Phonon Mechanism in Laser-Induced Ultrafast Demagnetization, *Phys. Rev. Lett.* **107**, 207201 (2011).
- [17] C. Illg, M. Haag, and M. Fähnle, Ultrafast demagnetization after laser irradiation in transition metals: *Ab initio* calculations of the spin-flip electron-phonon scattering with reduced exchange splitting, *Phys. Rev. B* **88**, 214404 (2013).
- [18] A. Baral, S. Vollmar, S. Kaltenborn, and H. C. Schneider, Re-examination of the Elliott–Yafet spin-relaxation mechanism, *New J. Phys.* **18**, 023012 (2016).
- [19] E. Carpene, E. Mancini, C. Dallera, M. Brenna, E. Puppini, and S. DeSilvestri, Dynamics of electron-magnon interaction and ultrafast demagnetization in thin iron films, *Phys. Rev. B* **78**, 174422 (2008).
- [20] A. Manchon, Q. Li, L. Xu, and S. Zhang, Theory of laser-induced demagnetization at high temperatures, *Phys. Rev. B* **85**, 064408 (2012).
- [21] M. Haag, C. Illg, and M. Fähnle, Role of electron-magnon scatterings in ultrafast demagnetization, *Phys. Rev. B* **90**, 014417 (2014).
- [22] E. G. Tveten, A. Brataas, and Y. Tserkovnyak, Electron-magnon scattering in magnetic heterostructures far out of equilibrium, *Phys. Rev. B* **92**, 180412(R) (2015).
- [23] M. Beens, R. A. Duine, and B. Koopmans, Modeling ultrafast demagnetization and spin transport: The interplay of spin-polarized electrons and thermal magnons, *Phys. Rev. B* **105**, 144420 (2022).
- [24] M. Haag, C. Illg, and M. Fähnle, Theory of scattering of crystal electrons at magnons, *Phys. Rev. B* **87**, 214427 (2013).
- [25] J. A. Hertz and D. M. Edwards, Electron-magnon interactions in itinerant ferromagnetism. I. Formal theory, *J. Phys. F: Met. Phys.* **3**, 2174 (1973).
- [26] M. C. T. D. Müller, S. Blügel, and C. Friedrich, Electron-magnon scattering in elementary ferromagnets from first principles: Lifetime broadening and band anomalies, *Phys. Rev. B* **100**, 045130 (2019).
- [27] E. Turgut, D. Zusin, D. Legut, K. Carva, R. Knut, J. M. Shaw, C. Chen, Z. Tao, H. T. Nembach, T. J. Silva, S. Mathias, M. Aeschlimann, P. M. Oppeneer, H. C. Kapteyn, M. M. Murnane, and P. Grychtol, Stoner versus Heisenberg: Ultrafast exchange reduction and magnon generation during laser-induced demagnetization, *Phys. Rev. B* **94**, 220408(R) (2016).
- [28] S. Eich, M. Plötzing, M. Rollinger, S. Emmerich, R. Adam, C. Chen, H. C. Kapteyn, M. M. Murnane, L. Plucinski, D. Steil, B. Stadtmüller, M. Cinchetti, M. Aeschlimann, C. M. Schneider, and S. Mathias, Band structure evolution during the ultrafast ferromagnetic-paramagnetic phase transition in cobalt, *Sci. Adv.* **3**, e1602094 (2017).
- [29] C. Dornes, Y. Acremann, M. Savoini, M. Kubli, M. J. Neugebauer, E. Abreu, L. Huber, G. Lantz, C. A. F. Vaz, H. Lemke, E. M. Bothschafter, M. Porer, V. Esposito, L. Rettig, M. Buzzi, A. Alberca, Y. W. Windsor, P. Beaud, U. Staub, D. Zhu *et al.*, The ultrafast Einstein–de Haas effect, *Nature (London)* **565**, 209 (2019).
- [30] S. R. Tauchert, M. Volkov, D. Ehberger, D. Kazenwadel, M. Evers, H. Lange, A. Donges, A. Book, W. Kreuzpaintner, U. Nowak, and P. Baum, Polarized phonons carry angular momentum in ultrafast demagnetization, *Nature (London)* **602**, 73 (2022).
- [31] B. Koopmans, M. van Kampen, and W. J. M. de Jonge, Experimental access to femtosecond spin dynamics, *J. Phys.: Condens. Matter* **15**, S723 (2003).
- [32] F. DallaLonga, J. T. Kohlhepp, W. J. M. de Jonge, and B. Koopmans, Influence of photon angular momentum on ultrafast demagnetization in nickel, *Phys. Rev. B* **75**, 224431 (2007).
- [33] G. P. Zhang, Y. H. Bai, and T. F. George, Spin berry points as crucial for ultrafast demagnetization, *Mod. Phys. Lett. B* **35**, 2150215 (2021).
- [34] Z. Chen and L.-W. Wang, Role of initial magnetic disorder: A time-dependent *ab initio* study of ultrafast demagnetization mechanisms, *Sci. Adv.* **5**, eaau8000 (2019).
- [35] W. Töws and G. M. Pastor, Many-Body Theory of Ultrafast Demagnetization and Angular Momentum Transfer in Ferromagnetic Transition Metals, *Phys. Rev. Lett.* **115**, 217204 (2015).
- [36] W. Töws, G. Stegmann, and G. M. Pastor, Spin and orbital symmetry breakings central to the laser-induced ultrafast demagnetization of transition metals, *Symmetry* **15**, 457 (2023).
- [37] K. Krieger, J. K. Dewhurst, P. Elliott, S. Sharma, and E. K. U. Gross, Laser-induced demagnetization at ultrashort time scales: Predictions of TDDFT, *J. Chem. Theory Comput.* **11**, 4870 (2015).
- [38] S. R. Acharya, V. Turkowski, G. P. Zhang, and T. S. Rahman, Ultrafast Electron Correlations and Memory Effects at Work: Femtosecond Demagnetization in Ni, *Phys. Rev. Lett.* **125**, 017202 (2020).
- [39] P. Scheid, S. Sharma, G. Malinowski, S. Mangin, and S. Lebègue, *Ab initio* study of helicity-dependent light-induced demagnetization: From the optical regime to the extreme ultraviolet regime, *Nano Lett.* **21**, 1943 (2021).
- [40] P. Elliott, A. Eschenlohr, J. Chen, S. Shallcross, U. Bovensiepen, J. K. Dewhurst, and S. Sharma, Transient spin injection efficiencies at ferromagnet/metal interfaces, *Adv. Mater. Interfaces* **9**, 2201233 (2022).
- [41] T. Barros, N. Tancogne-Dejean, J. Berakdar, and M. A. L. Marques, Impact of electron correlation on the light-induced demagnetization of elemental ferromagnetic metals, *Eur. Phys. J. B* **95**, 175 (2022).
- [42] S. Sharma, S. Shallcross, P. Elliott, and J. K. Dewhurst, Making a case for Femto-phono-magnetism with FePt, *Sci. Adv.* **8**, eabq2021 (2022).
- [43] G. P. Zhang and W. Hübner, Laser-Induced Ultrafast Demagnetization in Ferromagnetic Metals, *Phys. Rev. Lett.* **85**, 3025 (2000).
- [44] G. Stegmann, W. Töws, and G. M. Pastor, Ultrafast magnetization and energy flow in the laser-induced dynamics of transition metal compounds, *Phys. Rev. B* **107**, 054410 (2023).
- [45] B. Koopmans, H. Kicken, M. van Kampen, and W. de Jonge, Microscopic model for femtosecond magnetization dynamics, *J. Magn. Magn. Mater.* **286**, 271 (2005).
- [46] M. Krauß, T. Roth, S. Alebrand, D. Steil, M. Cinchetti, M. Aeschlimann, and H. C. Schneider, Ultrafast demagnetization

- of ferromagnetic transition metals: The role of the Coulomb interaction, *Phys. Rev. B* **80**, 180407(R) (2009).
- [47] S. Essert and H. C. Schneider, Electron-phonon scattering dynamics in ferromagnetic metals and their influence on ultrafast demagnetization processes, *Phys. Rev. B* **84**, 224405 (2011).
- [48] B. Y. Mueller and B. Rethfeld, Relaxation dynamics in laser-excited metals under nonequilibrium conditions, *Phys. Rev. B* **87**, 035139 (2013).
- [49] B. Y. Mueller, A. Baral, S. Vollmar, M. Cinchetti, M. Aeschlimann, H. C. Schneider, and B. Rethfeld, Feedback Effect during Ultrafast Demagnetization Dynamics in Ferromagnets, *Phys. Rev. Lett.* **111**, 167204 (2013).
- [50] D. M. Nenzo, B. Rethfeld, and H. C. Schneider, Particle-in-cell simulation of ultrafast hot-carrier transport in Fe/Au heterostructures, *Phys. Rev. B* **98**, 224416 (2018).
- [51] M. Beens, R. A. Duine, and B. Koopmans, *s-d* model for local and nonlocal spin dynamics in laser-excited magnetic heterostructures, *Phys. Rev. B* **102**, 054442 (2020).
- [52] S. Vollmar, K. Leckron, and H. C. Schneider, Ultrafast demagnetization dynamics due to electron-electron scattering and its relation to momentum relaxation in ferromagnets, [arXiv:2208.02356](https://arxiv.org/abs/2208.02356).
- [53] M. Beens, K. A. D. Mare, R. A. Duine, and B. Koopmans, Spin-polarized hot electron transport versus spin pumping mediated by local heating, *J. Phys.: Condens. Matter* **35**, 035803 (2022).
- [54] A. Baral and H. C. Schneider, Magnetic switching dynamics due to ultrafast exchange scattering: A model study, *Phys. Rev. B* **91**, 100402(R) (2015).
- [55] F. Töpler, J. Henk, and I. Mertig, Ultrafast spin dynamics in inhomogeneous systems: A density-matrix approach applied to Co/Cu interfaces, *New J. Phys.* **23**, 033042 (2021).
- [56] A. Suresh and B. K. Nikolic, Quantum-classical approach to spin and charge pumping and the ensuing radiation in the spintronics with example of ultrafast-light-driven weyl antiferromagnet Mn₃Sn, *Phys. Rev. B* **107**, 174421 (2023).
- [57] P.-W. Ma, S. L. Dudarev, and C. H. Woo, Spin-lattice-electron dynamics simulations of magnetic materials, *Phys. Rev. B* **85**, 184301 (2012).
- [58] M. Pankratova, I. P. Miranda, D. Thonig, M. Pereiro, E. Sjöqvist, A. Delin, O. Eriksson, and A. Bergman, Heat-conserving three-temperature model for ultrafast demagnetization in nickel, *Phys. Rev. B* **106**, 174407 (2022).
- [59] N. Kazantseva, U. Nowak, R. W. Chantrell, J. Hohlfeld, and A. Rebei, Slow recovery of the magnetisation after a sub-picosecond heat pulse, *Europhys. Lett.* **81**, 27004 (2008).
- [60] D. Zahn, F. Jakobs, Y. W. Windsor, H. Seiler, T. Vasileiadis, T. A. Butcher, Y. Qi, D. Engel, U. Atxitia, J. Vorberger, and R. Ernstorfer, Lattice dynamics and ultrafast energy flow between electrons, spins, and phonons in a 3d ferromagnet, *Phys. Rev. Res.* **3**, 023032 (2021).
- [61] D. Zahn, F. Jakobs, H. Seiler, T. A. Butcher, D. Engel, J. Vorberger, U. Atxitia, Y. W. Windsor, and R. Ernstorfer, Intrinsic energy flow in laser-excited 3d ferromagnets, *Phys. Rev. Res.* **4**, 013104 (2022).
- [62] U. Atxitia, O. Chubykalo-Fesenko, J. Walowski, A. Mann, and M. Münzenberg, Evidence for thermal mechanisms in laser-induced femtosecond spin dynamics, *Phys. Rev. B* **81**, 174401 (2010).
- [63] U. Atxitia, D. Hinzke, and U. Nowak, Fundamentals and applications of the Landau-Lifshitz-Bloch equation, *J. Phys. D: Appl. Phys.* **50**, 033003 (2017).
- [64] R. Rouzegar, L. Brandt, L. Nádvorník, D. A. Reiss, A. L. Chekhov, O. Gueckstock, C. In, M. Wolf, T. S. Seifert, P. W. Brouwer, G. Woltersdorf, and T. Kampfrath, Laser-induced terahertz spin transport in magnetic nanostructures arises from the same force as ultrafast demagnetization, *Phys. Rev. B* **106**, 144427 (2022).
- [65] B. Y. Mueller and B. Rethfeld, Thermodynamic μ t model of ultrafast magnetization dynamics, *Phys. Rev. B* **90**, 144420 (2014).
- [66] J. Kimling and D. G. Cahill, Spin diffusion induced by pulsed-laser heating and the role of spin heat accumulation, *Phys. Rev. B* **95**, 014402 (2017).
- [67] T. Griepe and U. Atxitia, Evidence of electron-phonon mediated spin flip as driving mechanism for ultrafast magnetization dynamics in 3d ferromagnets, *Phys. Rev. B* **107**, L100407 (2023).
- [68] Certain works can be assigned to several categories, for instance, extensions of the 3TM which are derived from a Boltzmann equation.
- [69] Z. Lin, L. V. Zhigilei, and V. Celli, Electron-phonon coupling and electron heat capacity of metals under conditions of strong electron-phonon nonequilibrium, *Phys. Rev. B* **77**, 075133 (2008).
- [70] P. Maldonado, K. Carva, M. Flammer, and P. M. Oppeneer, Theory of out-of-equilibrium ultrafast relaxation dynamics in metals, *Phys. Rev. B* **96**, 174439 (2017).
- [71] P. Scheid, G. Malinowski, S. Mangin, and S. Lebègue, *Ab initio* study of electronic temperature effects on magnetic materials properties, *Phys. Rev. B* **99**, 174415 (2019).
- [72] U. Ritzmann, P. M. Oppeneer, and P. Maldonado, Theory of out-of-equilibrium electron and phonon dynamics in metals after femtosecond laser excitation, *Phys. Rev. B* **102**, 214305 (2020).
- [73] C. D. Stanciu, F. Hansteen, A. V. Kimel, A. Kirilyuk, A. Tsukamoto, A. Itoh, and T. Rasing, All-Optical Magnetic Recording with Circularly Polarized Light, *Phys. Rev. Lett.* **99**, 047601 (2007).
- [74] I. Radu, K. Vahaplar, C. Stamm, T. Kachel, N. Pontius, H. A. Dürr, T. A. Ostler, J. Barker, R. F. L. Evans, R. W. Chantrell, A. Tsukamoto, A. Itoh, A. Kirilyuk, T. Rasing, and A. V. Kimel, Transient ferromagnetic-like state mediating ultrafast reversal of antiferromagnetically coupled spins, *Nature (London)* **472**, 205 (2011).
- [75] S. Mangin, M. Gottwald, C.-H. Lambert, D. Steil, V. Uhlř, L. Pang, M. Hehn, S. Alebrand, M. Cinchetti, G. Malinowski, Y. Fainman, M. Aeschlimann, and E. E. Fullerton, Engineered materials for all-optical helicity-dependent magnetic switching, *Nat. Mater.* **13**, 286 (2014).
- [76] G. Malinowski, F. D. Longa, J. H. H. Rietjens, P. V. Paluskar, R. Huijink, H. J. M. Swagten, and B. Koopmans, Control of speed and efficiency of ultrafast demagnetization by direct transfer of spin angular momentum, *Nat. Phys.* **4**, 855 (2008).
- [77] A. Melnikov, I. Razdolski, T. O. Wehling, E. T. Papaioannou, V. Roddatis, P. Fumagalli, O. Aktsipetrov, A. I. Lichtenstein, and U. Bovensiepen, Ultrafast Transport of Laser-Excited Spin-Polarized Carriers in Au/Fe/MgO(001), *Phys. Rev. Lett.* **107**, 076601 (2011).

- [78] T. Kampfrath, M. Battiato, P. Maldonado, G. Eilers, J. Nötzold, S. Mährlein, V. Zbarsky, F. Freimuth, Y. Mokrousov, S. Blügel, M. Wolf, I. Radu, P. M. Oppeneer, and M. Münzenberg, Terahertz spin current pulses controlled by magnetic heterostructures, *Nat. Nanotechnol.* **8**, 256 (2013).
- [79] G.-M. Choi, B.-C. Min, K.-J. Lee, and D. G. Cahill, Spin current generated by thermally driven ultrafast demagnetization, *Nat. Commun.* **5**, 4334 (2014).
- [80] G.-M. Choi and D. G. Cahill, Kerr rotation in Cu, Ag, and Au driven by spin accumulation and spin-orbit coupling, *Phys. Rev. B* **90**, 214432 (2014).
- [81] G.-M. Choi and B.-C. Min, Laser-driven spin generation in the conduction bands of ferrimagnetic metals, *Phys. Rev. B* **97**, 014410 (2018).
- [82] I. H. Shin, B. C. Min, B. K. Ju, and G. M. Choi, Ultrafast spin current generated by electron-magnon scattering in bulk of ferromagnets, *Jpn. J. Appl. Phys.* **57**, 090307 (2018).
- [83] A. Melnikov, L. Brandt, N. Liebing, M. Ribow, I. Mertig, and G. Woltersdorf, Ultrafast spin transport and control of spin current pulse shape in metallic multilayers, *Phys. Rev. B* **106**, 104417 (2022).
- [84] T. Lichtenberg, M. Beens, M. H. Jansen, B. Koopmans, and R. A. Duine, Probing optically induced spin currents using terahertz spin waves in noncollinear magnetic bilayers, *Phys. Rev. B* **105**, 144416 (2022).
- [85] P. Jiménez-Cavero, O. Gueckstock, L. Nádorník, I. Lucas, T. S. Seifert, M. Wolf, R. Rouzegar, P. W. Brouwer, S. Becker, G. Jakob, M. Kläui, C. Guo, C. Wan, X. Han, Z. Jin, H. Zhao, D. Wu, L. Morellón, and T. Kampfrath, Transition of laser-induced terahertz spin currents from torque-to conduction-electron-mediated transport, *Phys. Rev. B* **105**, 184408 (2022).
- [86] T. Seifert, S. Jaiswal, U. Martens, J. Hannegan, L. Braun, P. Maldonado, F. Freimuth, A. Kronenberg, J. Henrizi, I. Radu, E. Beaurepaire, Y. Mokrousov, P. M. Oppeneer, M. Jourdan, G. Jakob, D. Turchinovich, L. M. Hayden, M. Wolf, M. Münzenberg, M. Kläui *et al.*, Efficient metallic spintronic emitters of ultrabroadband terahertz radiation, *Nat. Photonics* **10**, 483 (2016).
- [87] T. S. Seifert, L. Cheng, Z. Wei, T. Kampfrath, and J. Qi, Spintronic sources of ultrashort terahertz electromagnetic pulses, *Appl. Phys. Lett.* **120**, 180401 (2022).
- [88] A. J. Schellekens, K. C. Kuiper, R. de Wit, and B. Koopmans, Ultrafast spin-transfer torque driven by femtosecond pulsed-laser excitation, *Nat. Commun.* **5**, 4333 (2014).
- [89] I. Rzdolski, A. Alekhin, N. Ilin, J. P. Meyburg, V. Roddatis, D. DIESING, U. Bovensiepen, and A. Melnikov, Nanoscale interface confinement of ultrafast spin transfer torque driving non-uniform spin dynamics, *Nat. Commun.* **8**, 15007 (2017).
- [90] S. Iihama, Y. Xu, M. Deb, G. Malinowski, M. Hehn, J. Gorchon, E. E. Fullerton, and S. Mangin, Single-shot multi-level all-optical magnetization switching mediated by spin transport, *Adv. Mater.* **30**, 1804004 (2018).
- [91] Q. Remy, J. Igarashi, S. Iihama, G. Malinowski, M. Hehn, J. Gorchon, J. Hohlfield, S. Fukami, H. Ohno, and S. Mangin, Energy efficient control of ultrafast spin current to induce single femtosecond pulse switching of a ferromagnet, *Adv. Sci.* **7**, 2001996 (2020).
- [92] J. Igarashi, Q. Remy, S. Iihama, G. Malinowski, M. Hehn, J. Gorchon, J. Hohlfield, S. Fukami, H. Ohno, and S. Mangin, Engineering single-shot all-optical switching of ferromagnetic materials, *Nano Lett.* **20**, 8654 (2020).
- [93] S. Iihama, Q. Remy, J. Igarashi, G. Malinowski, M. Hehn, and S. Mangin, Spin-transport mediated single-shot all-optical magnetization switching of metallic films, *J. Phys. Soc. Jpn.* **90**, 081009 (2021).
- [94] Q. Remy, J. Hohlfield, M. Vergès, Y. L. Guen, J. Gorchon, G. Malinowski, S. Mangin, and M. Hehn, Accelerating ultrafast magnetization reversal by non-local spin transfer, *Nat. Commun.* **14**, 445 (2023).
- [95] K. Jhuria, J. Hohlfield, A. Pattabi, E. Martin, A. Y. A. Córdova, X. Shi, R. L. Conte, S. Petit-Watelot, J. C. Rojas-Sanchez, G. Malinowski, S. Mangin, A. Lemaître, M. Hehn, J. Bokor, R. B. Wilson, and J. Gorchon, Spin-orbit torque switching of a ferromagnet with picosecond electrical pulses, *Nat. Electron.* **3**, 680 (2020).
- [96] T. A. Ostler, J. Barker, R. F. Evans, R. W. Chantrell, U. Atxitia, O. Chubykalo-Fesenko, S. E. Moussaoui, L. L. Guyader, E. Mengotti, L. J. Heyderman, F. Nolting, A. Tsukamoto, A. Itoh, D. Afanasiev, B. A. Ivanov, A. M. Kalashnikova, K. Vahaplar, J. Mentink, A. Kirilyuk, T. Rasing *et al.*, Ultrafast heating as a sufficient stimulus for magnetization reversal in a ferrimagnet, *Nat. Commun.* **3**, 666 (2012).
- [97] N. Berggaard, M. Hehn, S. Mangin, G. Lengaigne, F. Montaigne, M. L. M. Lalieu, B. Koopmans, and G. Malinowski, Hot-Electron-Induced Ultrafast Demagnetization in Co/Pt Multilayers, *Phys. Rev. Lett.* **117**, 147203 (2016).
- [98] A. L. Chekhov, Y. Behovits, J. J. F. Heitz, C. Denker, D. A. Reiss, M. Wolf, M. Weinelt, P. W. Brouwer, M. Münzenberg, and T. Kampfrath, Ultrafast Demagnetization of Iron Induced by Optical versus Terahertz Pulses, *Phys. Rev. X* **11**, 041055 (2021).
- [99] Q. Remy, Ultrafast spin dynamics and transport in magnetic metallic heterostructures, Ph.D. thesis, Université de Lorraine, 2021.
- [100] J. Simoni and S. Sanvito, Conservation of angular momentum in ultrafast spin dynamics, *Phys. Rev. B* **105**, 104437 (2022).
- [101] J. Igarashi, W. Zhang, Q. Remy, E. Díaz, J.-X. Lin, J. Hohlfield, M. Hehn, S. Mangin, J. Gorchon, and G. Malinowski, Optically induced ultrafast magnetization switching in ferromagnetic spin valves, *Nat. Mater.* (2023).
- [102] Ł. Cywiński and L. J. Sham, Ultrafast demagnetization in the sp-d model: A theoretical study, *Phys. Rev. B* **76**, 045205 (2007).
- [103] V. N. Gridnev, Ultrafast heating-induced magnetization switching in ferrimagnets, *J. Phys.: Condens. Matter* **28**, 476007 (2016).
- [104] G. D. Mahan, *Many-Particle Physics*, 3rd ed. (Springer, New York, 2000).
- [105] P. B. Allen, Theory of Thermal Relaxation of Electrons in Metals, *Phys. Rev. Lett.* **59**, 1460 (1987).
- [106] J. K. Chen, W. P. Latham, and J. E. Beraun, The role of electron-phonon coupling in ultrafast laser heating, *J. Laser Appl.* **17**, 63 (2005).

- [107] K. Blum, *Density Matrix Theory and Applications*, 3rd ed. (Springer, Berlin, 2012), Vol. 64.
- [108] P. Nieves, D. Serantes, U. Atxitia, and O. Chubykalo-Fesenko, Quantum Landau-Lifshitz-Bloch equation and its comparison with the classical case, *Phys. Rev. B* **90**, 104428 (2014).
- [109] J. Chen, D. Tzou, and J. Beraun, A semiclassical two-temperature model for ultrafast laser heating, *Int. J. Heat Mass Transfer* **49**, 307 (2006).
- [110] J. Pudell, M. Mattern, M. Hehn, G. Malinowski, M. Herzog, and M. Bargheer, Heat transport without heating?—an ultrafast x-ray perspective into a metal heterostructure, *Adv. Funct. Mater.* **30**, 2004555 (2020).
- [111] V. N. Gridnev, Ferromagneticlike states and all-optical magnetization switching in ferrimagnets, *Phys. Rev. B* **98**, 014427 (2018).
- [112] M.-L. Chavazas and Q. Remy, Time-dependent coherent light pulse absorption from macroscopic Maxwell equations, *Phys. Rev. B* **106**, 014310 (2022).
- [113] T. M. Philip and M. J. Gilbert, Theory of ac quantum transport with fully electrodynamic coupling, *J. Comput. Electron.* **17**, 934 (2018).
- [114] L. J. Cornelissen, K. J. H. Peters, G. E. W. Bauer, R. A. Duine, and B. J. van Wees, Magnon spin transport driven by the magnon chemical potential in a magnetic insulator, *Phys. Rev. B* **94**, 014412 (2016).
- [115] A. Rückriegel and R. A. Duine, Long-Range Phonon Spin Transport in Ferromagnet–Nonmagnetic Insulator Heterostructures, *Phys. Rev. Lett.* **124**, 117201 (2020).
- [116] A. J. Schellekens and B. Koopmans, Comparing Ultrafast Demagnetization Rates Between Competing Models for Finite Temperature Magnetism, *Phys. Rev. Lett.* **110**, 217204 (2013).
- [117] T. D. Cornelissen, R. Córdoba, and B. Koopmans, Microscopic model for all optical switching in ferromagnets, *Appl. Phys. Lett.* **108**, 142405 (2016).
- [118] L. Xu and S. Zhang, Magnetization dynamics at elevated temperatures, *J. Phys. E: Sci. Instrum.* **45**, 72 (2012).
- [119] L. Xu and S. Zhang, Self-consistent bloch equation and landau-lifshitz-bloch equation of ferromagnets: A comparison, *J. Appl. Phys.* **113**, 163911 (2013).
- [120] U. Bajpai, A. Suresh, and B. K. Nikolić, Quantum many-body states and green's functions of nonequilibrium electron-magnon systems: Localized spin operators versus their mapping to holstein-primakoff bosons, *Phys. Rev. B* **104**, 184425 (2021).
- [121] M. D. Stiles and A. Zangwill, Anatomy of spin-transfer torque, *Phys. Rev. B* **66**, 014407 (2002).
- [122] M. Beens, M. L. M. Laliu, A. J. M. Deenen, R. A. Duine, and B. Koopmans, Comparing all-optical switching in synthetic-ferrimagnetic multilayers and alloys, *Phys. Rev. B* **100**, 220409(R) (2019).
- [123] Y. L. W. van Hees, P. van de Meughevel, B. Koopmans, and R. Lavrijsen, Deterministic all-optical magnetization writing facilitated by non-local transfer of spin angular momentum, *Nat. Commun.* **11**, 3835 (2020).
- [124] P. Scheid, J. Hohlfeld, G. Malinowski, A. Bergman, O. Eriksson, S. Lebègue, and S. Mangin, Uncovering the role of the light-induced reduction of the inter-atomic exchange in the ultrafast demagnetization of Fe, Co, and Ni, [arXiv:2301.01055](https://arxiv.org/abs/2301.01055).
- [125] V. Korenman, J. L. Murray, and R. E. Prange, Local-band theory of itinerant ferromagnetism. I. Fermi-liquid theory, *Phys. Rev. B* **16**, 4032 (1977).